INS AIDING USING PASSIVE, BEARINGS-ONLY MEASUREMENTS OF AN UNKNOWN STATIONARY GROUND OBJECT

THESIS

Alec E. Porter, Second Lieutenant, USAF

AFIT/GE/ENG/03-15

DEPARTMENT OF THE AIR FORCE
AIR UNIVERSITY

AIR FORCE INSTITUTE OF TECHNOLOGY

Wright-Patterson Air Force Base, Ohio

The views expressed in this thesis are those of the author and do not reflect the official policy or position of the United States Air Force, Department of Defense, or the United States Government.

AFIT/GE/ENG/03-15

INS AIDING USING PASSIVE, BEARINGS-ONLY MEASUREMENTS OF AN UNKNOWN STATIONARY GROUND OBJECT

THESIS

Presented to the Faculty of the Graduate School of Engineering and Management
of the Air Force Institute of Technology
Air University
In Partial Fulfillment of the
Requirements for the Degree of
Master of Science

Alec E. Porter, B.S.
Second Lieutenant, USAF

March, 2003

AFIT/GE/ENG/03-15

INS AIDING USING PASSIVE, BEARINGS-ONLY MEASUREMENTS OF AN UNKNOWN STATIONARY GROUND OBJECT

Alec E. Porter, B.S.

Second Lieutenant, USAF

Approved:

M. Pachter	12 March 2003
Doctor Meir Pachter Thesis Advisor	Date
Peter S. Maybeck	12 March 2003
Doctor Peter Maybeck Committee Member	Date
	12 Mar 2003
Lieutenant Colonel Mikel Miller Committee Member	Date

Table of Contents

List of Figures

List of Tables

List of Symbols

Symbol Page

AFIT/GE/ENG/03-15

Abstract

The theory for Inertial Navigation System (INS) aiding using passive, bearings-only measurements of an unknown stationary ground object, in the vein of optical flow measurement, is developed. Stand-alone bearings-only measurements over time of an unknown, but stationary, ground object are shown to yield estimates of the aircraft's aerodynamic angles, viz., the angle of attack and sideslip angle. Two new equations containing the aircraft's angular navigation variables ψ, θ, ϕ, γ, H, and the aerodynamic angles are derived. This allows an update of the aircraft's attitude, thus making INS aiding using passive, bearings-only measurements possible. Moreover, the use of stadiametry, knowledge of the ground object's elevation, and an independent baro-altitude measurement yields an improved estimate of the aircraft's positional variables, thus completing the INS aiding task. At the same time, the geo-location of the observed ground object is also obtained. In addition, prior information on the position of the ground object further enhances the positional navigation variables' estimate, thus bringing to full fruition the favorable synergy of INS and bearings-only measurements of an unknown ground object.

INS AIDING USING PASSIVE, BEARINGS-ONLY MEASUREMENTS OF AN UNKNOWN STATIONARY GROUND OBJECT

I. Introduction

For centuries man has been on the move, crossing continents and oceans in search of adventure, riches, conquest, and scientific discovery. The simple act of moving from one place to another whether by foot, ship, or aircraft is often described as navigation.

Navigating the globe over the centuries has been accomplished using three different types of navigation: celestial, dead reckoning, and piloting. Celestial navigation is the process of computing position from the measured elevation angle of stars with respect to time; dead reckoning is the process of recording both the speed and direction of travel from the point of departure to produce a map of both the distance and the direction travelled; and piloting is the process of using known landmarks to estimate position [9].

The invention of the aircraft brought about new challenges to navigation. Celestial navigation worked only during clear nights while dead reckoning and piloting became increasingly difficult at high speeds and high altitudes. To overcome these problems, engineers turned to the laws of classical mechanics as described by Sir Isaac Newton. These laws tell us that an object in motion will stay in motion unless acted upon by an outside force. This force is known as acceleration, and it can be measured by an accelerometer [10]. In all truthfulness, accelerometers actually measure specific force, which is the acceleration measured by the sensor coupled with gravity. Accelerometers cannot distinguish between gravity and acceleration; thus

their attitude with respect to the earth, and a good model of the local gravity field, must be known in order to compensate for gravity and calculate the true acceleration. The attitude of the accelerometers can be determined from gyroscopes which measure angular rates. Accelerometers and gyroscopes form the backbone of the Inertial Navigation System (INS) which is essential in today's aircraft navigation systems.

The accelerations calculated from measurements provided by the accelerometers and gyroscopes provide both the position and the velocity of the aircraft. An INS does not require external measurements from other sources to operate. It is a completely self-contained measuring device; however, accurate knowledge of the initial INS position is required for precise navigation when all other errors in the system are neglected. Unfortunately, gyroscope measurement accuracy suffers from an error called drift which causes large position errors over long periods of time. To reduce or eliminate this problem, external measurements are often used to aid the INS in producing an accurate position estimation.

1.1 Background

1.1.1 History of Navigation. Successful navigation requires two things: a map which includes some kind of coordinate system to define position and some sort of measuring device which can be used to calculate a position. Early man used his own eyes as a measuring device and his memory as a map to navigate across the land using landmarks. As man began to travel farther and farther across the land and especially the seas, he developed maps and measuring devices to guide him. The Polynesians used celestial bodies to navigate the oceans over two thousand years ago [10], but not until the Eighteenth Century did man finally devise accurate means of navigating great distances over the earth's oceans.

Determining one's position with respect to latitude had been done for hundreds of years prior to the Eighteenth Century and could be done on any clear day or night with the help of a sextant, but determining longitude was a different matter.

The zero degree meridian of latitude is fixed on the earth at the equator but the zero degree meridian of longitude can be arbitrarily placed anywhere in the world (it resides in Greenwich, England today). More elegantly put, "The zero-degree parallel of latitude is fixed by the laws of nature, while the zero-degree meridian of longitude shifts like the sands of time [2]." To determine one's longitude at sea, the time at the point of departure versus the time aboard the ship needs to be known with a great deal of precision. The differences in time according to the clocks combined with the know latitude can be converted into the distance traversed longitudinally.

Pendulous clocks of the early Eighteenth Century were not accurate nor robust enough to keep precise time aboard a ship at sea. So pressing was the need to develop accurate seafaring clocks that the British Parliament passed the Longitude Act of 1714 offering a prize of £20,000 (worth several million dollars in 1990 money) to anyone who could solve the problem [2].

A simple clockmaker by the name of John Harrison succeeded where so many before him had failed. He designed a pendulous-free, highly accurate mechanical clock driven by springs and resembling a pocket watch. His invention forever changed navigation and "accomplished what Newton had feared impossible: He invented a clock that would carry the true time from home port, like an eternal flame, to any remote corner of the world [2]."

Newton's name would also be associated with another milestone in navigation history. The laws of mechanics and gravitation which Newton had defined nearly two centuries earlier would form the theoretical basis for the design of the sensors that would make inertial navigation possible in the middle of the Twentieth Century [10].

Many of the theories behind inertial navigation were well known before the middle of the Twentieth Century, but it wouldn't be until World War II that Germany's V-2 rockets would successfully use inertial sensors [10] to guide their deadly cargo to London. The Cold War also hastened the development of highly accurate

INS's to guide long-range bombers and ICBMs, but the INS has also found its way into peaceful applications such as commuter flight and landing men safely on the moon.

1.1.2 Inertial Navigation System. Inherent to all INS are two main components, the Inertial Measurement Unit (IMU) and the navigation computer. The IMU often consists of three accelerometers and three gyroscopes mounted in orthogonal triads that measure specific force and angular rates respectively. The raw measurement data from the IMU is sent to the navigation computer which determines the acceleration from the specific force, angular rate measurements, and a model of the local gravity field. The computer then uses the acceleration information to calculate the position and velocity, while gyros provide the attitude of the IMU. The IMU and navigation computer are collocated in the same box for easy installation and replacement [8].

Modern flight systems rely on an INS because it is a completely self-contained, nonjammable system that provides redundancy for other flight systems that can experience interference (i.e., radar), but the system does suffer form the unbounded growth of errors in position over time. These errors are caused by misalignment of the INS before takeoff and sensor imperfections that include accelerometer bias and gyroscope drift [9]. Therefore, an INS typically uses some form of position and velocity aiding from external sensors such as radar and more recently GPS.

1.1.3 Aided INS. The unbounded errors found in an INS can be reduced either by building more accurate accelerometers and gyroscopes or by aiding the system externally with position and/or velocity measurements. The cost of very accurate sensors is often too high for the desired application and there is a physical limit to the accuracy of the sensors, so many engineers have turned to external measuring devices to aid the INS.

There are many different systems available to aid the INS, including but not limited to:

1. Doppler Velocity Sensors (DVS).
2. Tactical Air Navigation (TACAN).
3. Global Positioning Systems (GPS.)
4. Forward Looking Infrared (FLIR) and Line-of-Sight (LOS) to a waypoint.

The measurements from these aiding systems along with the data output form the INS are combined mathematically in a Kalman filter [8] to produce an estimate of the aircraft's position. The Kalman filter "is simply an optimal recursive data processing algorithm" [4] derived by R. E. Kalman in 1960.

All four of the above-mentioned aiding systems improve INS long term operation, but they all have major drawbacks. DVS and TACAN require active sensors (i.e., radio pulses) to operate. The major drawbacks to active sensing are the sensor's susceptibility to jamming and disclosure of the aircraft's position while in operation. GPS is a passive system, thus an aircraft using GPS will not disclose its position, but this system also has some major drawbacks. GPS signals can be jammed or spoofed with inexpensive and low-power devices, degrading the system's accuracy. FLIR and LOS require fixed, known ground objects to calculate position, a major drawback when an aircraft is operating over unknown or hostile territory. A system consisting of passive measurements, impervious to jamming or spoofing, that could aid the INS without knowledge of known ground objects would provide INS error correction without any of the disadvantages as described above.

1.2 Problem Definition

The main thrust of this research is to develop the theory and mathematics behind aiding an INS with passive, bearings-only measurements of unknown ground objects. Passive refers to the use of sensors that don't emit radiation; thus the

aircraft cannot be tracked. Bearings-only simply refers to LOS measurements that display the direction of the unknown ground object with respect to the body of the aircraft; no velocity, acceleration, or distance measurements are made by the sensor. A ground object is any stationary object that the pilot or the passive sensor can easily acquire and track. The ground object does not need to be man-made; however, man-made objects are often easy to spot and track.

Passive, bearings-only measurements of an unknown, but stationary, ground object used to aid an INS produces a completely autonomous, self-contained navigation system. The system cannot be jammed or spoofed and does not rely on any external measurement sources to operate. The system can be integrated into any aircraft that has the capabilities of taking passive, bearings-only measurements from either pilot or automatic input.

1.3 Summary of Current Knowledge

The idea of using unknown ground objects to aid an INS was first proposed by engineers at NASA for use in the Apollo Lunar Module (LM) [1]. The idea was to aid the LM's navigation computer when the LM was on both the light and dark side of the moon. The mathematical framework for a two-dimensional scenario was created for the project but it was never used in the Apollo's navigation system.

To understand how the system would have worked, assume an astronaut is able to track an unknown ground object as in Figure 1.1. The navigation system must rely on the changes in the tracking angle α_c, where the subscript c denotes a calculation based on sensor measurements, and the distance S_0 of the LM from the ground object to compute the vehicle's velocity vector. The equations that determine the tracking angle and velocity vector were developed by Alexander Koso at the MIT Instrumentation Laboratory [1].

The idea was reexamined forty years later by Murat Polat, a Lieutenant in the Turkish Air Force studying in the United States at the Air Force Institute of

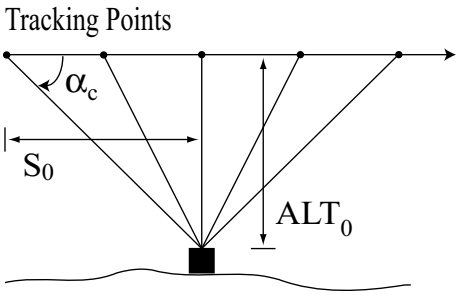

Figure 1.1 NASA Measurement Scenario

Technology (AFIT) for his thesis [7] on INS aiding. He examined a similar two-dimensional scenario involving aircraft dynamics. The major difference in the two research efforts is the type of measurements used to determine position. Koso assumed the distance to the ground object could be determined while Murat focused on bearings-only measurements and the aircraft's navigation variables. The mathematical framework developed by Alexander Koso and Murat Polat is examined more in-depth in Chapter 2.

1.4 Scope

Reference [7] has shown that in a limited two-dimensional case, INS aiding with passive bearings-only measurements is possible. This research will take the algorithm developed for the two-dimensional measurement case and expand them into a more realistic and practical three-dimensional case. This will allow the INS aiding algorithm to handle "real world" aircraft operations better. The algorithm will be tested using a wide variety of simulated aircraft flight profiles. The aiding concept is still in the theoretical stage and no field testing of an actual system will occur.

1.5 Assumptions

The inertial velocity vector of the aircraft is assumed to be linear during all measurements, thus precluding the pilot from performing any maneuvers. Although

restrictive, the total measurement interval required to produce aiding information is less than one minute for most cases as outlined in Chapter 4. When aiding is desired, the minimal time it takes to produce reliable measurements for the aiding algorithm will not have a negative impact on the operation of the aircraft for most cases. To insure the non-radiating capability of the INS aiding sensor, bearings-only measurements are taken by an optical or electro-optical tracker.

1.6 Methodology

The same approach used by [7] is incorporated in this research but expanded into three-dimensional space. There is a total of nine measurement variables available from the aircraft's instrumentation. Four of these measurements are positional variables and include the initial position of the aircraft (X_0, Y_0, Z_0) as well as the aircraft's velocity (V). The other five measurements are angular variables and include the Euler Angles of the aircraft (yaw $\equiv \psi$, pitch $\equiv \theta$, roll $\equiv \phi$) as well as the heading (H) and the flight path angle (γ) of the aircraft. The bearings-only measurements are used to calculate the angle γ_D, where the subscript D differentiates this angle measurement from the flight path angle γ, between the inertial velocity vector and the initial LOS vector. Figure 1.2 shows the three-dimensional measurement scenario. The measurement scenario begins at X_0, Y_0, and Z_0 with an initial LOS measurement to the unknown but stationary ground object P. The path of the aircraft is along the inertial velocity vector $\vec{V}$ described by H and γ in the reference frame (X, Y, Z). The orientation of the aircraft with respect to the inertial velocity vector is described by X_b, Y_b, and Z_b where X_b points directly out of the noise of the aircraft, Y_b is perpendicular to the aircraft's fuselage and oriented along the right wing, and Z_b is orientated perpendicular to the bottom of the aircraft. The angle measured between two consecutive LOS measurements is σ, and the calculated angle between the inertial velocity vector and the initial LOS measurement is γ_D. The

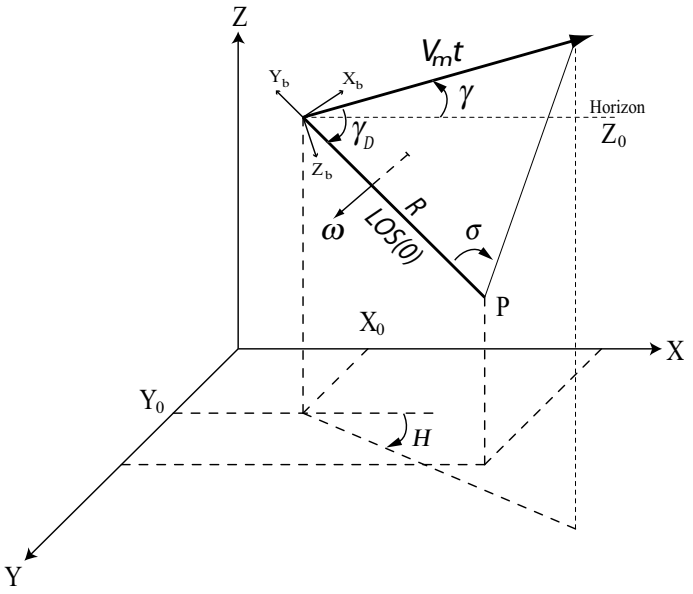

Figure 1.2 3-D Measurement Scenario

vector $\vec{\omega}$ describes the orientation of the plane formed by the inertial velocity vector and the LOS vector with respect to the (X, Y, Z) frame.

The nine measurement variables are used to estimate the angles α and β that describe the orientation of the inertial velocity vector with respect to the aircraft's body axes. These angles are often described as the kinematic angle of attack and the kinematic sideslip angle respectively [3].

1.7 Summary

The goal of this research is to expand upon the knowledge of INS aiding using passive, bearings-only measurements of an unknown, but stationary, ground object as shown in [7]. This is accomplished through the creation and extensive testing of the three-dimensional aiding algorithm outlined in Chapter 3. MatLab® is used to produce realistic flight simulations to show that this approach to INS aiding will produce an accurate and reliable navigation solution. In addition to aiding the INS, the algorithm in Chapter 3 is used to determine the position of the unknown ground object.

II. Theory

2.1 Introduction

This chapter provides the theory behind INS aiding and using passive, bearings-only measurements to accomplish the same. The chapter begins with a brief overview of INS aiding and then goes into the theory and mathematics developed by [7] for the two-dimensional scenario. The chapter ends with a discussion of the theory and mathematics behind expanding the two-dimensional scenario into three dimensions.

2.2 INS Aiding

There are a wide variety of systems both onboard the aircraft and external that are used for aiding. External systems include GPS, radio navigation aids, ground-based radar, and star trackers. Onboard systems include altimeters, Doppler radar, airspeed indicators, magnetic sensors, and electro-optical imaging systems [10]. The aiding concept proposed by [7] and the subject of this research is an onboard optical or electro-optical system.

Regardless of the system, they all operate on the same basic principle. The INS outputs the desired navigation measurements. The navigation measurements used during aiding are usually position and velocity, but the INS can also output acceleration and attitude information. The measurements from the INS are compared to the output signals of the independent navigation aid - see, e.g., Figure 2.1. This information is then sent to a filter for processing. A Kalman Filter is often used to weight the incoming information to generate state estimates and send corrections to the INS. These corrections help the overall system achieve a more accurate navigation solution [10].

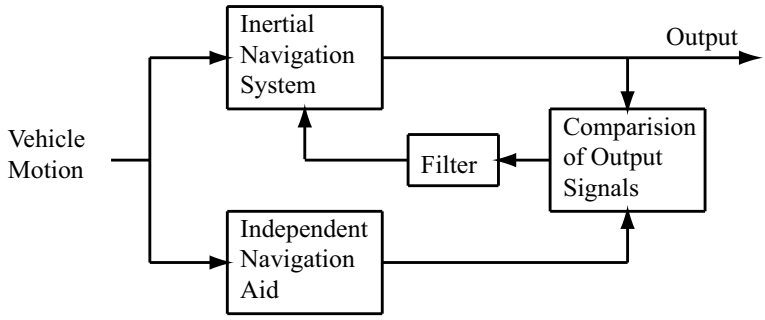

Figure 2.1 INS Aiding Principle

2.3 Two-Dimensional Aiding Concepts

2.3.1 The Apollo Scenario. The use of unknown ground objects to aid an INS was first proposed for use on the Lunar Module (LM) in the Apollo moon missions. Reference [1] outlined the two-dimensional case shown in Figure 2.2. The

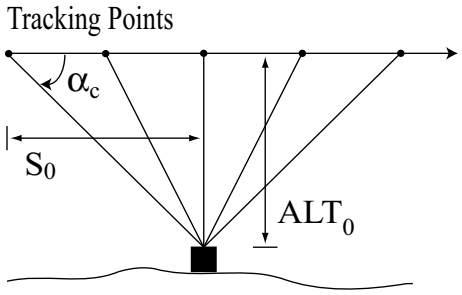

Figure 2.2 Lunar Tracking Scenario

angle α_c can easily be found by solving $\cot \alpha_c = S_0/ALT_0$, where ALT_0 is the height of the LM above the unknown landmark. The subscript c refers to the computed angle α from S_0 and ALT_0. Unfortunately, this equation neglects several key factors. First, the LM is assumed to be stationary in the above equation. The movement of the LM around the curved surface of the moon causes a variation in the measured bearing angle. This variation is accounted for by taking the LM's angular velocity ω_0 and multiplying by the LM's height above the center of the moon r_0 to produce a linear velocity. The linear velocity is then multiplied by the time τ for the measurement interval to establish the variation in the bearing angle due to the orbit of the LM.

The computed bearing measurement now becomes

$$\cot \alpha_c = \frac{S_0 - r_0 w_0 \tau}{ALT_0} \tag{2.1}$$

Second, errors in measurements must be taken into account. There is some uncertainty in the altitude of the LM denoted by $r(t_0)$, and uncertainty in the altitude of the landmark denoted by ΔALT. The actual bearing measurement denoted with the subscript α is

$$\cot \alpha_\alpha = \frac{S_0 - r_0 w_0 \tau}{ALT_0 + r(t_0) - \Delta ALT} + \frac{\cot \alpha(0)(r(t_0) - \Delta ALT)}{ALT_0 + r(t_0) - \Delta ALT} \tag{2.2}$$

where $\alpha(0)$ is the initial LOS measurement. The movement of the LM also produces velocity errors in both the horizontal and vertical directions as shown in Figure 2.3.

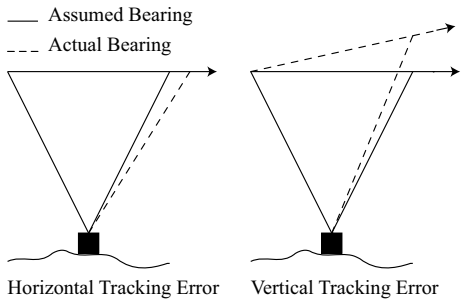

Figure 2.3 Velocity Tracking Errors

The computed bearing measurement with vertical errors becomes:

$$\cot \alpha_\alpha = \frac{S_0 - r_0 \omega_0 \tau}{ALT_0 + \dot{r}(t_0)\tau} \tag{2.3}$$

The computed bearing measurement with horizontal errors becomes:

$$\cot \alpha_\alpha = \frac{S_0 - (\omega_0 + \omega(t_0)) r_0 \tau}{ALT_0} \tag{2.4}$$

The final error source that is taken into account is the initial range error $\theta(t_0)$. The initial range error is due to the determination of the velocity error in Equation (2.3) and causes an angle between the LM's assumed and actual path. It is impossible to distinguish the initial range error from the velocity error, and the effect of this error is shown in Figure 2.4.

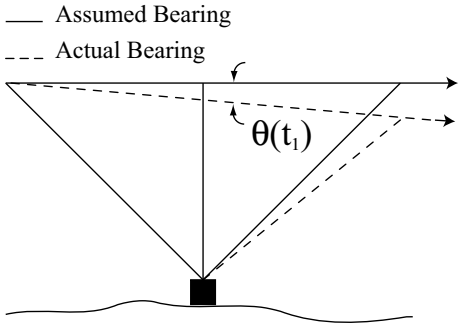

Figure 2.4 Initial Range Error

The computed bearing measurement with the initial range error becomes

$$\cot \alpha_\alpha = \frac{S_0 - r_0\omega_0\tau}{ALT_0 - \theta(t_0)r_0\omega_0\tau} \tag{2.5}$$

where (t_0) represents the initial time of the measurement scenario.

The above equations provide the background required to determine the position error for INS aiding. The errors terms are generally small, so linear approximation techniques are applied. A more in-depth explanation of the techniques used to determine the position error can be found in [1] or [7]. The difference between the actual bearing angle α_α and the computed bearing angle α_c is written as

$$\begin{aligned} \cot \alpha_\alpha - \cot \alpha_c \approx \tfrac{1}{ALT_0^2}(r_0\omega_0[r(t_0) - \Delta ALT] + S_0[r_0\omega_0\theta(t_0) - r(t_0)])\tau \\ + \tfrac{r_0\omega_0}{ALT_0^2}[\dot{r}(t_0) - r_0\omega_0\theta(t_0)]\tau^2 \end{aligned} \tag{2.6}$$

The angle β between the assumed and the actual bearing measurement is written as

$$\sin\beta \approx \frac{\phi r_0 \tau}{ALT_0 + r(t_0) - \Delta ALT + (r(t_0) - r_0\omega_0\theta(t_0))\tau} \tag{2.7}$$

where ϕ is the position error. Depending on the orbit of the LM, $(r(t_0) - r_0\omega_0\theta(t_0))$ will be negligible. Using small angle approximation and the assumption that $(r(t_0) - r_0\omega_0\theta(t_0))$ can indeed be neglected, Equation (2.7) is rewritten as:

$$\phi \approx \frac{\beta(t)(ALT_0 + r(t_0) - \Delta ALT)}{r_0 t} \tag{2.8}$$

The orbital parameters of the LM can now be found using Equation (2.6) and Equation (2.8) without the knowledge of the ground object's position; however, four lunar landmarks must be tracked to determine the initial condition errors [1].

2.3.2 The Aircraft Scenario. The bearings-only concept for INS aiding was never used in any of the Apollo missions but it did provide insight for [7] who would revisit the idea some forty years later. There are some key differences between the work done in [1] and [7]. As stated earlier, [1] assumed the altitude of the LM and its distance to the landmark were known; however, [7] was interested in the case in which the only measurements available for INS aiding were bearings-only LOS measurements taken by some sort of passive sensor which does not provide ranging information. This forced [7] to look at the aiding concept in a new mathematical light. Reference [7] also examined a two-dimensional case; however, the dynamics behind aircraft flight offered unique challenges that the LM did not need to face.

Figure 2.5 shows the measurements scenario used by [7] to construct the mathematics required for INS aiding. The body frame of the aircraft (x_b, y_b) relative to the velocity vector $\vec{V}$ can be described by the angle α'. Reference [7] theorized that the angle α' is related to the aircraft's angular navigation variables yaw ψ, pitch θ, roll ϕ, dive angle γ, and heading H. The angles σ_0 through σ_3 are measured

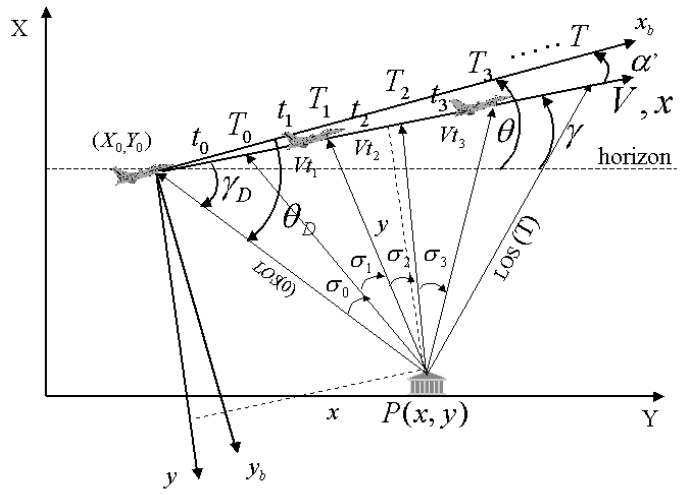

Figure 2.5 Aircraft Tracking Scenario [7]

using the passive sensor while the angle γ_D is calculated from those measurements. The aircraft provides a measurement of scaler velocity and the bearings-only measurements are taken at time intervals of t_k for $k = 0, 1, ..., N$ over a total time T. The angle included between the initial LOS to the ground object and the aircraft's inertial velocity vector is denoted by γ_D. This section is concerned with the estimate of γ_D. Figure 2.5 shows the two-dimensional measurement geometry used in [6] and [7] to derive the mathematics required for INS aiding.

The LOS angle increments σ_0 through σ_k are directly measured using the passive optical sensor while the angle γ_D is calculated from those measurements using a batch calculation. The bearings-only measurements are taken at time intervals of t_k for $k = 0, 1, ..., N$ over a total time T. The current time is related to the time intervals through the following equation

$$T_k = \sum_{i=0}^{k} t_i \ . \tag{2.9}$$

The following geometric argument is used. A circumscribing circle is drawn through two consecutive measurement points and the unknown landmark P at (x, y) as shown in Figure 2.6. Such a circumscribing circle can be drawn for every pair of

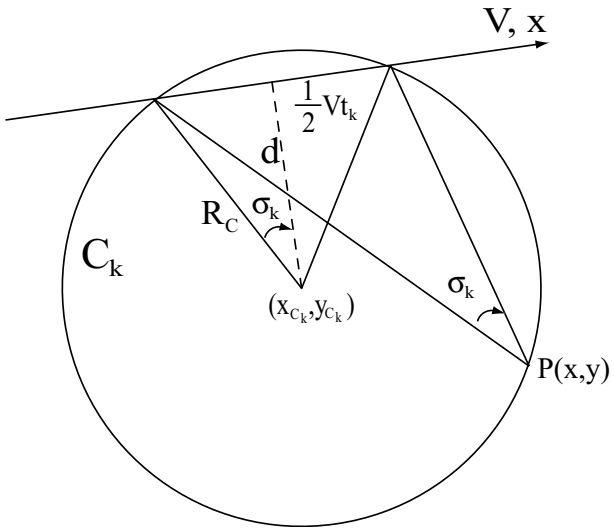

Figure 2.6 Geometry of Bearing-Only Measurements

consecutive measurement points, producing $N + 1$ circles intersecting at the point P. The aircraft's velocity is V and the radius of the circle C_k is

$$R_k = \frac{Vt_k}{2\sin\sigma_k},\ k = 0, 1, ..., N \tag{2.10}$$

with the (x, y) center of the circle C_k located at

$$\begin{aligned} x_{C_k} &= \sum_{i=0}^{k} Vt_i - \tfrac{1}{2}Vt_k \\ y_{C_k} &= \tfrac{Vt_k}{2\tan\sigma_k},\ k = 1, ..., N \end{aligned} \tag{2.11}$$

and the center of the "prime" circle C_0 at

$$x_{C_0} = \frac{1}{2}Vt_0 \ \text{ and } \ y_{C_0} = \frac{Vt_0}{2\tan\sigma_0} \tag{2.12}$$

The equations of the of the circles are written in the form $x^2+y^2=R^2$. The "prime" circle equation becomes

$$(x-\frac{1}{2}Vt_0)^2+(y-\frac{Vt_0}{2\tan\sigma_0})^2=\frac{V^2t_0^2}{4\sin^2\sigma_0} \tag{2.13}$$

and the equation representing the rest of the circles becomes

$$(x-\sum_{i=0}^{k}Vt_i+\frac{1}{2}Vt_k)^2+(y-\frac{Vt_k}{2\tan\sigma_k})^2=\frac{V^2t_k^2}{4\sin^2\sigma_k} \tag{2.14}$$

Subtracting Equation (2.13) from Equation (2.14) while substituting in T_k as defined in Equation (2.9) yields the linear homogeneous system of N equations in x, y, and V:

$$(2T_k-t_k-t_0)x+(t_k\cot\sigma_k-t_0\cot\sigma_0)y-T_k(T_k-t_k)V=0 \tag{2.15}$$

The linear homogeneous system of N equations is represented in matrix notation by $H\theta=0$, where θ is the parameter vector $[x\ \ y\ \ V]^T$, and the $N\times 3$ regressor matrix

$$H=\begin{bmatrix} 2T_1-t_1-t_0 & t_1\cot\sigma_1-t_0\cot\sigma_0 & -T_1(T_1-t_1) \\ \vdots & \vdots & \vdots \\ 2T_N-t_N-t_0 & t_N\cot\sigma_N-t_0\cot\sigma_0 & -T_N(T_N-t_N) \end{bmatrix}_{N\times 3} \tag{2.16}$$

The regressor matrix H is constructed from measurements taken by the passive sensor at deterministic time intervals. A Singular Value Decomposition (SVD) of H leads to a solution for γ_D as follows.

The SVD of H is in the form

$$H=U\Sigma V^T$$

where U is a $N\times N$ matrix, Σ is a "diagonal" $N\times 3$ matrix, and V is 3×3. As expected, the first two diagonal elements of Σ are several orders of magnitude greater

than the third diagonal element; thus, Σ is reduced to a diagonal 2×2 matrix, and to maintain proper dimensions, both U and V^T are reduced to $N \times 2$ and 2×3 matrices, respectively. This yields the reduced matrices

$$\underline{H} = \underline{U\Sigma}^{1/2} \text{ and } K = \underline{\Sigma}^{1/2}\underline{V}^T$$

It is now apparent that $H = \underline{H}K$; thus, a full rank factorization of the regressor matrix H is performed. Defining $\underline{\theta} = K\theta$ produces $K\theta = 0$, a reduced linear homogeneous system of two independent equations in the three unknowns x, y, and V:

$$\begin{aligned} K_{1,1}x + K_{1,2}y + K_{1,3}V = 0 \\ K_{2,1}x + K_{2,2}y + K_{2,3}V = 0 \end{aligned} \tag{2.17}$$

This yields the solution

$$x = K_x V \text{ and } y = K_y V \tag{2.18}$$

where the "gains"

$$K_x = \frac{K_{1,2}K_{2,3} - K_{1,3}K_{2,2}}{K_{1,1}K_{2,2} - K_{1,2}K_{2,1}} \text{ and } K_y = \frac{K_{1,3}K_{2,1} - K_{1,1}K_{2,3}}{K_{1,1}K_{2,2} - K_{1,2}K_{2,1}} \tag{2.19}$$

Evidently, x and y are homogeneous in V. Now, the angle

$$\gamma_D = \arctan(y/x)$$

The SVD yields the "gains" K_x and K_y and, in view of Equation (2.18), the angle γ_D included between the initial LOS measurement and the inertial velocity vector is

$$\gamma_D = \arctan(K_y/K_x)$$

The "clean" K_x and K_y parameters are the result of the SVD of the regressor matrix H in Equation (2.16). Referring back to Figure 2.5, the equation $\theta_D - \gamma_D = \theta - \gamma$

relates the optical bearing measurements to the angular navigation variables and makes INS aiding using passive, bearings-only measurements a reality.

2.4 The Three-Dimensional Aiding Concept

Maintaining the autonomy of the INS is paramount. Hence, it is envisioned that passive, bearings-only measurements of a unknown, but stationary, ground object provided by, e.g., an optical or electro-optical tracker will be used. Indeed, assuming an unknown ground object is tantamount to confining the navigation system to the measurement of optical flow. Optical flow is the apparent motion of luminance patterns in images caused by the motion of physical objects in the scene, or the self-movement of the sensor. In this respect, the four scenarios to consider when tracking a stationary object on the ground from the air for the purpose of updating the INS are:

1. The ground object is a high intensity point source, e.g., a heat source. Infrared (IR) trackers provide an automated means of tracking the point source.
2. There is an intermediate level of intensity/luminance variation in the scene being viewed. Specialized video equipment can automatically track a point in the scene, an implementation of an optical flow sensor.
3. There are low intensity variations in the observed scene. A human operator is needed to close the tracking loop through the use of optical tracking equipment such as a telescope or a driftmeter.
4. In very low SNR conditions the ground object may be impossible to track, i.e. cloud cover or night-time flight over water.

The INS aiding method developed in this paper is applicable to the first three scenarios.

In this paper it is assumed that the position of the ground object is unknown and that the measurements made by the optical sensor are bearings-only, removing

the requirement of range information; however, multiple observations of the ground object are made. The bearings-only measurements are taken by a tracker consisting of a precision telescope mounted on a gimballed system. This allows the operator controlled sensor to remain pointed to the ground object independent of the aircraft's motion. The direction of the line of sight to the ground object relative to the body axes of the aircraft is measured with pickoffs that are attached to the gimbals. It is envisioned that the inertial angular rate of the line of sight measurement is directly determined with a two-degrees-of-freedom rate gyro whose spin axis is aligned with the optical axis of the telescope so that the gyros' input axes and the sensor's optical axis form a triad of orthogonal axes. The gyro should be of medium quality, so as not to pick up the earth rate.

Indeed, and with hindsight, the origins of the INS aiding concept developed in this paper can be traced back to the driftmeter [11]. A driftmeter is a navigational instrument out of the past, from the days when the navigator's station was in the glassed nose of the aircraft. A navigator's driftmeter, or cinemoderivometer in Europe, is a camera like instrument pointed straight towards the ground with a built in scale in the focal plane. The length of the scale is equal to the focal length of the objective. The scale is rotated and the angle of rotation measured. Selecting a stationary object on the ground and rotating the eyepiece so the object moved parallel to the scale gives the drift angle. Measuring the time for the object to move between the two lines at the front and end of the scale is used to calculate the ground speed of the aircraft if its altitude is known; the ground speed being the altitude divided by the time it takes the ground object to travel between the two lines at the front and back of the scale . Indeed, the INS passive aiding methodology developed in this paper can be viewed as a modern development of the venerable driftmeter navigational aid. In this paper, the general optical flow-based INS aiding theory is developed and validated.

2.5 Summary

This chapter provides an overview of the theory and background in the special two-dimensional INS aiding case using passive, bearings-only measurements of an unknown, but stationary, ground object. The general concept for aiding the INS in three dimensions is also provided above. The next chapter will expand the research presented in [7] into the three-dimensional world where the mathematics become increasingly more complex. The concepts which build the three-dimensional case are also dealt with in greater detail.

III. Modeling Methodology

3.1 Overview

This chapter provides the theory used to generate flight profiles to test and evaluate the passive, bearing-only measurement concept for INS aiding. The chapter begins by explaining the relationships between the measurements taken by the passive sensor and the aircraft's navigation variables. These relationships show the feasibility of aiding an INS using passive, bearings-only measurements. Next, the theory and mathematics involved in updating the INS position are discussed and derived. Finally, the algorithm that makes aiding and geo-location possible is derived.

3.2 Analysis

The kinematic measurement scenario where bearings-only measurements of an unknown landmark are taken over time is considered. First, it is shown that a stand-alone optical sensor measures the angles α' and β' included between the aircraft's inertial velocity vector $\vec{V}$ and the body of the aircraft - see, e.g., Figure 3.1. Specifically, the estimates of a) γ_D, the angle included between the aircraft's

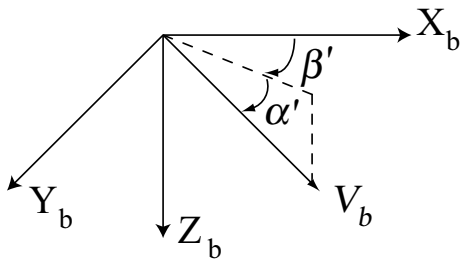

Figure 3.1 "Aerodynamic" Angles

inertial velocity vector and the initial LOS to the ground object - see, e.g., Fig 2.5, b) $\vec{\omega}_1$, the unit vector which is the rate of the LOS to the ground object - see, e.g., Figure 3.3, and, c) the angles ψ_{LOS} and θ_{LOS} included between the initial LOS to the ground object and the aircraft's body axes - see, e.g., Figure 3.2, are provided

by the optical sensor. The angles γ_D, ω_1, ψ_{LOS}, and θ_{LOS} and are related to the "aerodynamic" angles α' and β'. Hence, the "aerodynamic" angles of the aircraft can be calculated from the optical flow measurement.

The air speed of the aircraft is equal to its ground speed in the absence of wind. Thus, by definition, in the absence of wind the aerodynamic angles α and β then satisfy

$$\alpha = \alpha'$$
$$\beta = \beta'$$

Hence, it is fair to say that the bearings-only measurements of an unknown ground object afford the estimation of the aircraft's aerodynamic angles.

3.2.1 The Main Equation. The Line of Sight (LOS) vector $\overrightarrow{LOS}$ is specified with respect to the body frame by the angles ψ_{LOS} and θ_{LOS} as seen in Figure 3.2.

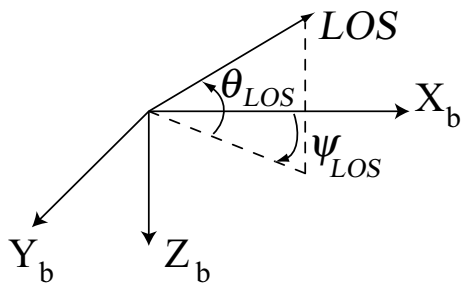

Figure 3.2 *LOS* in the Body Frame

The unit LOS vector resolved in the body frame is

$$\overrightarrow{LOS}_{1b} = \begin{bmatrix} \cos\theta_{LOS} \cdot \cos\psi_{LOS} \\ \cos\theta_{LOS} \cdot \sin\psi_{LOS} \\ \sin\theta_{LOS} \end{bmatrix} \tag{3.1}$$

Consider the plane P formed by the aircraft's velocity vector $\vec{V}$ and the initial LOS vector $\overrightarrow{LOS}_1$ to the unknown ground object P - see, e.g., Figure 3.3. The angular rate $\vec{\omega}$ of the LOS from the aircraft to the unknown landmark is in the plane

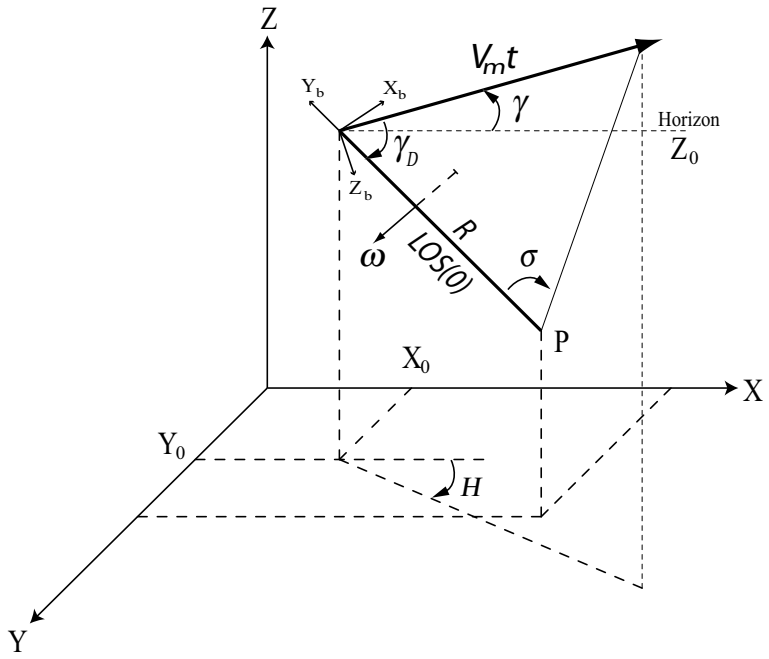

Figure 3.3 Measurement Scenario

perpendicular to the LOS; thus, $\vec{\omega}$ will always contain a component of zero along the LOS. If, during the measurement interval t, the aircraft is flying with a constant velocity, then $\vec{\omega}$ is also perpendicular to the plane P. The LOS angle in the plane P is represented by σ with the magnitude of the angular rate represented by $\dot{\sigma}$. The LOS angular rate $\dot{\sigma}$, and the spatial orientation of the plane P relative to the navigation frame are obtained from the two measured nonzero components of $\vec{\omega}$. Measurements of $\vec{\omega}$ resolved in the telescope's frame are provided by an optical tracker consisting of a precision telescope mounted on a gimbal system. $\vec{\omega}$ is transformed into the aircraft's body frame using the gimbals' angles readings.

The vectors $\vec{\omega}$, $\vec{V}$, and $\overrightarrow{LOS}$ from Figure 3.3 are related through the cross product

$$\vec{V} \times \overrightarrow{LOS} = |V||LOS| \sin \gamma_D \frac{\vec{\omega}}{\|\omega\|} \tag{3.2}$$

where the unit vector

$$\vec{\omega}_1 = \frac{\vec{\omega}}{\|\omega\|}$$

Note: $\|\omega\| = |\dot{\sigma}|$ and γ_D is the angle included between the velocity vector and the initial LOS. Dividing both sides of Equation (3.2) by $|V||LOS|$ produces the equation

$$\vec{V}_1 \times \overrightarrow{LOS}_1 = \vec{\omega}_1 \sin\gamma_D \tag{3.3}$$

where $\vec{V}_1$, $\overrightarrow{LOS}_1$, and $\vec{\omega}_1$ are all unit vectors. Equation (3.3) is referred to as the "Main Equation" because it relates the five angular navigation variables with the measurements of the optical tracker: $\vec{\omega}_1$, $\overrightarrow{LOS}_1$, and the calculated angle γ_D, the latter being derived from the LOS angle measurements σ.

Representing the "Main Equation" in the body frame yields

$$\vec{V}_{1b} \times \overrightarrow{LOS}_{1b} = \sin\gamma_D \vec{\omega}_{1b} \tag{3.4}$$

Substituting Equations (3.12) and (3.1) into Equation (3.4) yields Equation (3.5).

$$\sin\gamma_D \cdot \vec{\omega}_{1b} = \begin{bmatrix} \cos\alpha'\cos\beta' \\ \cos\alpha'\sin\beta' \\ \sin\alpha' \end{bmatrix} \times \begin{bmatrix} \cos\theta_{LOS}\cos\psi_{LOS} \\ \cos\theta_{LOS}\sin\psi_{LOS} \\ \sin\theta_{LOS} \end{bmatrix} \tag{3.5}$$

The cross product is expanded to produce

$$MC_n^b \begin{bmatrix} \cos\gamma\cos H \\ \cos\gamma\sin H \\ -\sin\gamma \end{bmatrix} = \sin\gamma_D \begin{bmatrix} \omega_x \\ \omega_y \\ \omega_z \end{bmatrix} \tag{3.6}$$

where the matrix M is defined in Equation (3.7).

$$M = \begin{bmatrix} 0 & \sin\theta_{LOS} & -\cos\theta_{LOS}\sin\psi_{LOS} \\ -\sin\theta_{LOS} & 0 & \cos\theta_{LOS}\cos\psi_{LOS} \\ \cos\theta_{LOS}\sin\psi_{LOS} & -\cos\theta_{LOS}\cos\psi_{LOS} & 0 \end{bmatrix} \tag{3.7}$$

Note that M is singular and $M^T = -M$. ω_x, ω_y, and ω_z are components of the unit vector $\vec{\omega}_1$ resolved in the body frame.

A direct relationship, albeit not explicit, is now established between the five angular navigation variables ψ, θ, ϕ, H, and γ, and the optical measurements ω_x, ω_y, ω_z, γ_D, ψ_{LOS}, and θ_{LOS}. The singularity of the 3×3 matrix M should come as no surprise - as expected, two new measurement equations are established.

3.2.2 Two-Dimensional Verification. It is illuminating to consider the special two-dimensional case. The special two-dimensional geometry using the three-dimensional derivation is recovered by setting H, ψ, and ϕ to zero and only using θ and γ. In the two-dimensional case, ψ_{LOS} and the z component of ω are zero. Figure 3.4 represents the two-dimensional case. In the two-dimensional case the

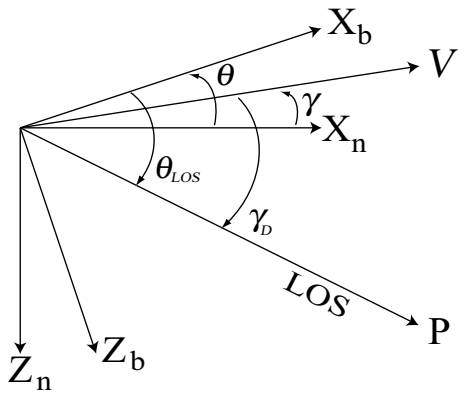

Figure 3.4 2-D Measurement Scenario

angular navigation variables are θ and γ and the optical measurements are θ_{LOS} and γ_D,which is derived from the LOS and σ measurements. It is apparent from the figure that

$$\theta_{LOS} - \gamma_D = \theta - \gamma \tag{3.8}$$

Careful examination of Equation (3.3) reveals that $\vec{\omega}_1$ points in the negative y direction and is zero in both the x and z direction. Thus, the unit angular rate vector is specified by $\omega_y = -1$. For the two-dimensional case, the "Main Equation"

is thus

$$MC_n^b \begin{bmatrix} \cos\gamma \\ 0 \\ -\sin\gamma \end{bmatrix} = \sin\gamma_D \begin{bmatrix} 0 \\ -1 \\ 0 \end{bmatrix}$$

where M is reduced to

$$\begin{bmatrix} 0 & \sin\theta_{LOS} & 0 \\ -\sin\theta_{LOS} & 0 & \cos\theta_{LOS} \\ 0 & -\cos\theta_{LOS} & 0 \end{bmatrix}$$

and C_n^b is reduced to

$$\begin{bmatrix} \cos\theta & 0 & -\sin\theta \\ 0 & 1 & 0 \\ \sin\theta & 0 & \cos\theta \end{bmatrix}$$

Hence, the "Main Equation" yields

$$\begin{bmatrix} 0 \\ \sin(\theta - \gamma - \theta_{LOS}) \\ 0 \end{bmatrix} = \begin{bmatrix} 0 \\ -\sin\gamma_D \\ 0 \end{bmatrix}$$

confirming that the three-dimensional equations produce the measurement equation (3.8), as expected. The new measurement Equation (3.8) relates the optical measurements and the relevant angular navigation variables. It is a linear regression in γ and θ, thus making possible enhanced estimates of the aircraft's angular navigation variables; however, these enhancements do not directly translate into improvements in the estimate of the aircraft's positional navigation variables.

3.2.3 Aerodynamic Angles Relationships. The aerodynamic angles α' and β' are related to the five angular navigation variables of the aircraft, viz., its Euler angles ψ, θ, ϕ and its course H and flight path angle γ. The navigation variables ψ, θ,

and ϕ are the aircraft's Euler angles that represent yaw, pitch, and roll respectively - see, e.g., Figure 3.5. The navigation variables γ and H are the angles used to specify

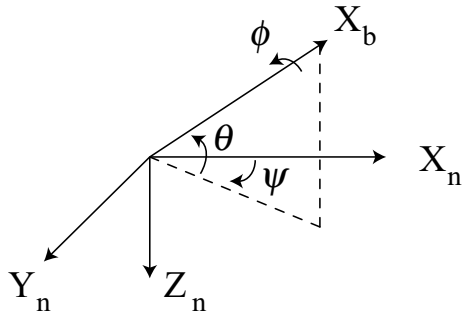

Figure 3.5 Euler Angles

the velocity vector in the navigation frame shown in Figure 3.6.

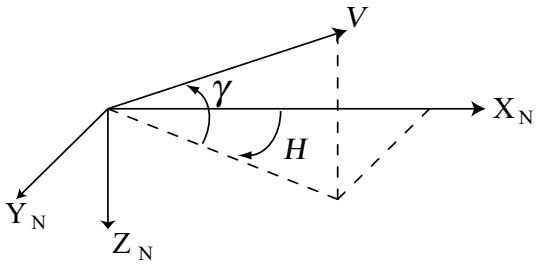

Figure 3.6 Velocity Vector

The orientation of the body frame with respect to the navigation frame is specified by the Euler angles ψ, θ, and ϕ. The Direction Cosine Matrix (DCM) C_b^n transforms vectors resolved in the body frame of the aircraft into vectors resolved in the navigation frame according to Equation (3.9). Conversely, the transpose of C_b^n, C_n^b, takes information from the navigation frame and transforms it into the body frame.

$$C_b^n = \begin{bmatrix} \cos\psi\cos\theta & \cos\psi\sin\theta\sin\phi - \sin\psi\cos\phi & \cos\psi\sin\theta\cos\phi + \sin\psi\sin\phi \\ \sin\psi\cos\theta & \sin\psi\sin\theta\sin\phi + \cos\psi\cos\phi & \sin\psi\sin\theta\cos\phi - \cos\psi\sin\phi \\ -\sin\theta & \cos\theta\sin\phi & \cos\theta\cos\phi \end{bmatrix} \quad (3.9)$$

The unit velocity vector $\vec{V}_1$ is in the direction of the aircraft's inertial velocity vector and is specified with respect to the navigation frame by the angles γ and H as shown in Figure 3.6, and therefore is

$$\vec{V}_{1n} = \begin{bmatrix} \cos\gamma\cos H \\ \cos\gamma\sin H \\ -\sin\gamma \end{bmatrix} \tag{3.10}$$

Hence, in the body frame

$$\vec{V}_{1b} = C_n^b \begin{bmatrix} \cos\gamma\cos H \\ \cos\gamma\sin H \\ -\sin\gamma \end{bmatrix} \tag{3.11}$$

The aircraft's unit inertial velocity vector is also represented in the body frame by the "aerodynamic" angles α' and β' - see, e.g., Figure 3.1 - yielding the equation

$$\vec{V}_{1b} = \begin{bmatrix} \cos\alpha'\cos\beta' \\ \cos\alpha'\sin\beta' \\ \sin\alpha' \end{bmatrix} \tag{3.12}$$

Equations (3.11) and (3.12) are combined into Equation (3.13) to show the relationship between the angles α' and β' and the five navigation variables ψ, θ, ϕ, γ, and H:

$$\begin{bmatrix} \cos\alpha'\cos\beta' \\ \cos\alpha'\sin\beta' \\ \sin\alpha' \end{bmatrix} = C_n^b \begin{bmatrix} \cos\gamma\cos H \\ \cos\gamma\sin H \\ -\sin\gamma \end{bmatrix} \tag{3.13}$$

This yields two independent equations relating the aerodynamic angles α' and β' to the five angular navigation variables ψ, θ, ϕ, γ, and H.

One can explicitly express the "aerodynamic" angles α' and β' as a function of the five angular navigation variables ψ, θ, ϕ, H, and γ. From Equation (3.13)

$$\sin\alpha' = \sin\theta\cos\gamma\cos\phi\cos(\psi - H) + \cos\gamma\sin\phi\sin(\psi - H) - \cos\theta\sin\gamma\cos\phi \quad (3.14)$$

Equation (3.13) also yields the following two relationships

$$\begin{aligned}\cos\alpha'\cos\beta' &= [\cos\psi\cos\theta,\ \sin\psi\cos\theta,\ -\sin\theta]\cdot[\cos\gamma\cos H,\ \cos\gamma\sin H,\ -\sin\gamma]^T \\ &= \cos\theta\cos\gamma\cos(\psi - H) + \sin\theta\sin\gamma\end{aligned}$$

and

$$\begin{aligned}\cos\alpha'\sin\beta' = [&\cos\psi\sin\theta\sin\psi - \sin\psi\cos\phi\ , \sin\psi\sin\theta\sin\phi + \cos\psi\cos\phi, \cos\theta\sin\phi] \\ &\cdot[\cos\gamma\cos H,\ \cos\gamma\sin H,\ -\sin\gamma]^T \\ &= \sin\theta\cos\gamma\sin\phi\cos(\gamma - H) - \cos\gamma\cos\phi\sin(\gamma - H) - \sin\gamma\cos\theta\sin\phi\end{aligned}$$

Dividing $\cos\alpha'\cos\beta'$ by $\cos\alpha'\sin\beta'$ yields Equation (3.15).

$$\tan\beta' = \frac{\sin\theta\cos\gamma\sin\phi\cos(\psi - H) - \cos\gamma\cos\phi\sin(\psi - H) - \sin\gamma\cos\theta\sin\phi}{\cos\theta\cos\gamma\cos(\psi - H) + \sin\theta\sin\gamma} \quad (3.15)$$

3.2.4 The Special Two-Dimensional Case. The relationships between the aerodynamic angles and the angular navigation variables is easily seen in the special two dimensional case. Consider an aircraft flying wings level at a constant speed. There are two cases to consider.

1.) Flight in the vertical plane: only the pitch angle, θ, is considered. For this case, the Euler angles ψ and ϕ are set to zero. The aircraft's pitch angle θ is determined solely from the flight path angle γ; thus H and β' are set to zero. The first case is illustrated in Figure 3.7. It is clear from Figure 3.7 that $\alpha' = \theta - \gamma$.

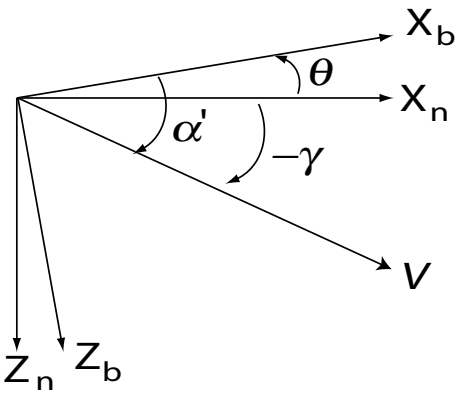

Figure 3.7 α' Relationship

Substituting in $\psi = \phi = 0$, $H = 0$, and $\beta' = 0$ into Equation (3.13) yields

$$\begin{bmatrix} \cos\alpha' \\ 0 \\ \sin\alpha' \end{bmatrix} = \begin{bmatrix} \cos\theta & 0 & -\sin\theta \\ 0 & 1 & 0 \\ \sin\theta & 0 & \cos\theta \end{bmatrix} \begin{bmatrix} \cos\gamma \\ 0 \\ -\sin\gamma \end{bmatrix}$$

Multiplying everything out produces three equations

$$\begin{aligned} \cos\alpha' &= \cos\theta\cos\gamma + \sin\theta\sin\gamma \\ 0 &= 0 \\ \sin\alpha' &= \sin\theta\cos\gamma - \cos\theta\sin\gamma \end{aligned}$$

that are reducible to

$$\begin{aligned} \cos\alpha' &= \cos(\theta - \gamma) \\ \sin\alpha' &= \sin(\theta - \gamma) \end{aligned}$$

Thus, the measurement equation is obtained

$$\alpha' = \theta - \gamma \tag{3.16}$$

2.) Flight in the horizontal plane: only the heading angle, ψ, is considered. For this case, the Euler angles ϕ and θ are set to zero. The aircraft's course H is

determined solely from the heading ψ; thus γ and α' are set to zero. The second case is illustrated in Figure 3.8. It is clear from Figure 3.8 that $\beta' = H - \psi$. Substituting

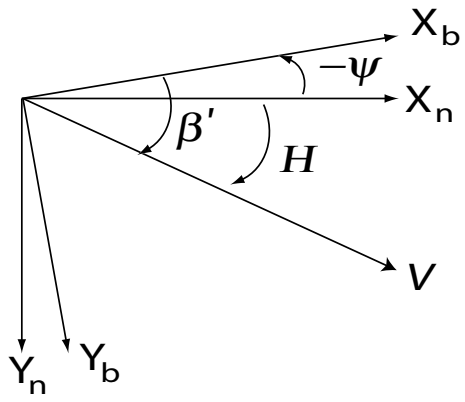

Figure 3.8 β' Relationship

in $\phi = \theta = 0$, $\gamma = 0$, and $\alpha' = 0$ into Equation (3.13) yields

$$\begin{bmatrix} \cos\beta' \\ \sin\beta' \\ 0 \end{bmatrix} = \begin{bmatrix} \cos\psi & \sin\psi & 0 \\ -\sin\psi & \cos\psi & 0 \\ 0 & 0 & 1 \end{bmatrix} \begin{bmatrix} \cos H \\ \sin H \\ 0 \end{bmatrix}$$

Multiplying everything out produces three equations

$$\begin{aligned} \cos\beta' &= \cos\psi\cos H + \sin\psi\cos H \\ \sin\beta' &= -\sin\psi\cos H + \cos\psi\sin H \\ 0 &= 0 \end{aligned}$$

that are reducible to

$$\begin{aligned} \cos\beta' &= \cos(H - \psi) \\ \sin\beta' &= \sin(H - \psi) \end{aligned}$$

Thus, the measurement equation is obtained

$$\beta' = H - \psi \tag{3.17}$$

The INS aiding algorithm in this paper assumes that the aircraft flies wings level so that the "aerodynamic" angles α' and β' are small. The simplified measurement Equations (3.16) and (3.17) can only be used under these small angle assumptions. In other words, for the simplified Equations (3.16) and (3.17) to hold during a INS aiding run, the aircraft must be flown wings level and at a constant altitude.

3.2.5 The Aerodynamic Angles Measurement. One can express α' and β' directly as a function of the optical measurements ψ_{LOS}, θ_{LOS}, ω_x, ω_y, ω_z, and γ_D. From Equation (3.6)

$$\omega_x \sin\gamma_D = \sin\theta_{LOS}\cos\alpha'\sin\beta' - \cos\theta_{Los}\sin\psi_{LOS}\sin\alpha'$$

$$\omega_y \sin\gamma_D = \sin\theta_{LOS}\cos\alpha'\cos\beta' + \cos\theta_{Los}\cos\psi_{LOS}\sin\alpha'$$

Rearranging and subtracting those two equations yields

$$\begin{aligned}\sin^2\theta_{LOS}\cos^2\alpha' = \sin^2\gamma_D(\omega_x^2+\omega_y^2) + \cos^2\theta_{LOS}\sin^2\alpha + \\ 2\sin\alpha\sin\gamma_D\cos\theta_{LOS}\cdot(\omega_x\sin\psi_{LOS} - \omega_y\cos\psi_{LOS})\end{aligned}$$

Solving for $\sin\alpha'$ yields.

$$\begin{aligned}\sin\alpha' = &-\sin\gamma_D\cos\theta_{LOS}(\omega_x\sin\psi_{LOS} - \omega_y\cos\psi_{LOS}) \pm \\ &\sqrt{\begin{array}{c}\sin^2\gamma_D\cos^2\theta_{LOS}(\omega_x\sin\psi_{LOS} - \omega_y\cos\psi_{LOS}) \\ +\sin^2\theta_{LOS} - (\omega_x^2+\omega_y^2)\sin^2\gamma_D\end{array}}\end{aligned}$$

The two-dimensional special case dictates the use of the + sign and not the − sign. Hence,

$$\begin{aligned}\sin\alpha' = &\sqrt{\begin{array}{c}\sin^2\gamma_D\cos^2\theta_{LOS}(\omega_x\sin\psi_{LOS} - \omega_y\cos\psi_{LOS}) \\ +\sin^2\theta_{LOS} - (\omega_x^2+\omega_y^2)\sin^2\gamma_D\end{array}} \\ &-\sin\gamma_D\cos\theta_{LOS}(\omega_x\sin\psi_{LOS} - \omega_y\cos\psi_{LOS})\end{aligned} \tag{3.18}$$

Rearranging and dividing the two equations derived from Equation (3.6) yields a solution for β' in the form

$$\tan\beta' = \frac{\cos\theta_{LOS}\sin\psi_{LOS}\sin\alpha' + \omega_x \sin\gamma_D}{\cos\theta_{LOS}\cos\psi_{LOS}\sin\alpha' + \omega_y \sin\gamma_D} \tag{3.19}$$

The angles α' and β' are now expressed as functions of the five angular navigation variables ψ, θ, ϕ, γ, and H in Equations (3.14) and (3.15), and the measurements ψ_{LOS}, θ_{LOS}, γ_D, ω_x, and ω_y in Equations (3.18) and (3.19). Combining Equations (3.18) and (3.14), and Equations (3.15) and (3.19) yields the two new measurement equations provided by the optical flow measurement.

$$\begin{aligned} z_1 &\stackrel{\Delta}{=} \sqrt{\sin^2\gamma_D\cos^2\theta_{LOS}(\eta)^2 + \sin^2\theta_{LOS} - (\omega_x^2+\omega_y^2)\sin^2\gamma_D} - \eta\sin\gamma_D\cos\theta_{LOS} \\ &= \sin\theta\cos\gamma\cos\phi\cos(\psi-H) + \cos\gamma\sin\phi\sin(\psi-H) - \cos\theta\sin\gamma\cos\phi \end{aligned} \tag{3.20}$$

where $\eta = \omega_x\sin\psi_{LOS} - \omega_y\cos\psi_{LOS}$

$$z_2 \stackrel{\Delta}{=} \frac{\cos\theta_{LOS}\sin\psi_{LOS}\sin\alpha'+\omega_x\sin\gamma_D}{\cos\theta_{LOS}\cos\psi_{LOS}\sin\alpha'+\omega_y\sin\gamma_D} = \frac{\sin\theta\sin\phi\cos(\psi-H)-\cos\phi\sin(\psi-H)-\tan\gamma\cos\theta\sin\phi}{\cos\theta\cos(\psi-H)+\sin\theta\tan\gamma} \tag{3.21}$$

The two Equations (3.20) and (3.21) are equivalent to Equation (3.6). More importantly, in the process of developing Equations (3.20) and (3.21), the aerodynamic angles are directly expressed in terms of optical flow measurements, refereing to Equations (3.18) and (3.19).

The angles α' and β' are related to the five angular navigation variables according to Equation (3.13). Hence, using Equations (3.18) and (3.19) to affirm that a stand-alone optical flow sensor provides a means to update the aircraft's angular navigation variables, viz., the aircraft's attitude.

3.2.5.1 Special Cases. Assume that the flight path profile flown during the INS update run is such that θ, γ, ϕ, and $|H-\psi|$ are small, in which case the RHS of Equations (3.20) and (3.21) are simplified and the two measurement

equations are

$$z_1 \approx \cos\phi\,[\sin\theta\cos\gamma\cos(\psi - H) - \cos\theta\sin\gamma]$$
$$z_2 \approx \tfrac{\cos\phi}{\cos\theta}\tan(H - \psi)$$

Alternatively, assume that the flight profile flown during the INS update run calls for an overflight of the ground object, in which case $\phi = \psi = H = 0$, $\omega_x = \omega_z = 0$, and $\omega_y = -1$. Equation (3.20) yields the single measurement equation

$$\theta_{LOS} - \gamma_D = \theta - \gamma$$

Also note: during level flight, when $\gamma = 0$,

$$z_1 = \sin\theta\cos\phi\cos(H - \psi) + \sin\phi\sin(\psi - H)$$
$$z_2 = \tan\theta\tan\phi + \tfrac{\cos\phi}{\cos\theta}\tan(\psi - H)$$

and θ, ϕ, $|H - \psi|$ small, imply that

$$z_1 \approx \sin\theta \;\text{ and }\; z_2 \approx \tan(\psi - H)$$

i.e.,

$$\alpha' \approx \theta \;\text{ and }\; \beta' \approx H - \psi$$

as expected.

The results obtained so far lay the foundation for updating the INS angular navigation variables. These results are summarized in

Theorem 1: Consider the kinematic measurement scenario in Figure (3.9), where bearing measurements on a stationary ground object whose position is not known, are taken over time. It is then possible to estimate the angles which specify the direction of the aircraft's inertial velocity vector V relative to the body axes, viz., the "aerodynamic" angles α' and β'.

□

Proof: see the development in Section 3.2.5.

Proposition 2: The aerodynamic angles α' and β' are related to the aircraft's five angular navigation variables ψ, θ, ϕ, γ, and H.

□

Proof: see the development in Section 3.2.3 and 3.2.4.

Theorem 1 and Proposition 2 are exploited to lay the foundation for INS-aiding using bearings-only measurements as stated in

Theorem 3: The kinematic measurement scenario which entails bearings-only measurements over time on a stationary ground object whose position is not known, yields two new independent measurement equations featuring the aircraft's five angular navigation variables ψ, θ, ϕ, γ, and H. Hence, the optical measurements can be used to update the INS provided attitude estimate.

□

3.3 INS Aiding - Angular Navigation Variables

Updating the INS-provided angular navigation variables in the case where the aircraft flies wings level and at a constant speed is based on the measurement Equations (3.20) and (3.21). In the special two dimensional case, one reverts to Equation (3.8) where the aircraft overflies the ground object. The measurement is

$$z = \theta_{LOS_{meas}} - \gamma_{D_{meas}} \tag{3.22}$$

where

$$\gamma_{D_{meas}} = \gamma_D + \upsilon_3 \text{ and } \theta_{LOS_{meas}} = \theta_{LOS} + \upsilon_2 \tag{3.23}$$

with the υ_2 and υ_3 noise statistics modeled as zero-mean normal distributions. Substituting Equation (3.23) into Equation (3.22) yields the new measurement equation:

$$z = \theta_{LOS} + \upsilon_2 - \gamma_D - \upsilon_3 \tag{3.24}$$

Equation (3.24) is equivalent to

$$z = \theta - \gamma + \upsilon_6 \tag{3.25}$$

where $\upsilon_6 = \upsilon_2 - \upsilon_3$.

The INS provides estimates of θ and γ in the form

$$\hat{\gamma}^- = \gamma + \upsilon_4 \text{ and } \hat{\theta}^- = \theta + \upsilon_5 \tag{3.26}$$

with the υ_4 and υ_5 noise statistics modeled as zero-mean normal distributions. The superscript - indicates a value determined at a time before the measurement incorporation, while the superscript + indicates the same value after the measurement incorporation [4]. Equations (3.25) and (3.26) are combined to obtain the linear regression for angular navigation variables aiding:

$$\begin{bmatrix} \hat{\theta}^- \\ \hat{\gamma}^- \\ z \end{bmatrix} = \begin{bmatrix} 1 & 0 \\ 0 & 1 \\ 1 & -1 \end{bmatrix} \begin{bmatrix} \theta \\ \gamma \end{bmatrix} + \begin{bmatrix} \upsilon_4 \\ \upsilon_5 \\ \upsilon_6 \end{bmatrix} \tag{3.27}$$

The linear regression (3.27) is in the standard form

$$Z = HX + V$$

where

$$X = \begin{bmatrix} \theta \\ \\ \gamma \end{bmatrix}, \; H = \begin{bmatrix} 1 & 0 \\ 0 & 1 \\ 1 & -1 \end{bmatrix}, \text{ and } V = \begin{bmatrix} \upsilon_4 \\ \upsilon_5 \\ \upsilon_6 \end{bmatrix}$$

and is solved using the Minimum Variance formulae [4]

$$\begin{aligned} \hat{X}^+ &= \left[H^T R_{noise}^{-1} H\right]^{-1} H^T R_{noise}^{-1} Z \\ P^+ &= \left[H^T R_{noise}^{-1} H\right]^{-1} \end{aligned} \tag{3.28}$$

where $\hat{X}^+$ is the minimum variance parameter estimate and P^+ is the predicted parameter estimation error covariance matrix. The equation error covariance matrix is

$$R_{noise} = \begin{bmatrix} \sigma_{\upsilon_4}^2 & 0 & 0 \\ 0 & \sigma_{\upsilon_5}^2 & 0 \\ 0 & 0 & \sigma_{\upsilon_6}^2 \end{bmatrix}$$

$\hat{X}^+$ provides the updated estimate of the aircraft's angular navigational variables θ and γ. In summary, stand alone optical flow measurements are conducive to updating the INS's angular navigation variables.

3.4 Ins Aiding - Positional Navigation Variables

3.4.1 Transformation. INS aiding using passive, bearings-only measurements of an unknown ground object requires transforming position vectors resolved in the plane P as shown in Figure 3.9, into position vectors resolved in the navigation frame. The initial position of the aircraft is (X_0, Y_0, Z_0). The velocity of the aircraft is described by the heading angle H and the flight path angle γ. The range of the LOS vector to the unknown point P is R. The unknown point P in the navigation frame is (X_P, Y_P, Z_P). The plane P is constructed from the velocity vector and the LOS vector. The plane exists in two-dimensional space using the (x, y) coordinate system. The orientation of P with respect to the navigation frame is described by

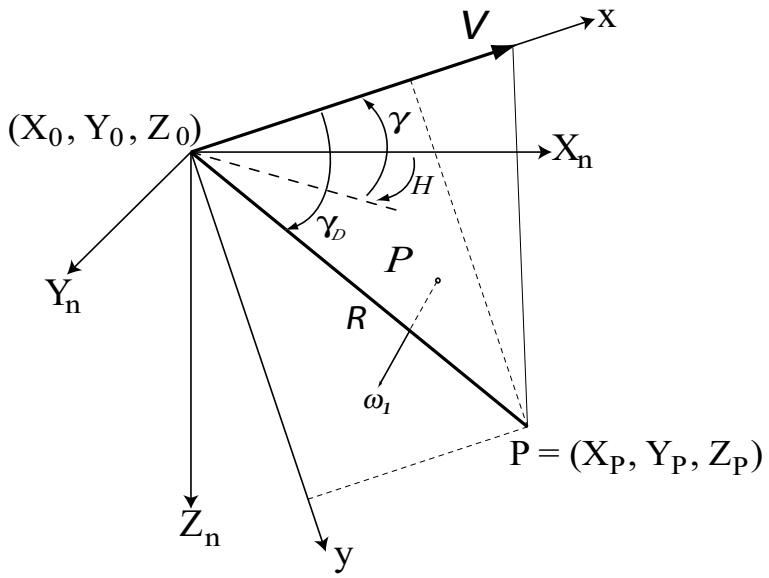

Figure 3.9 Measurement Scenario

the unit vector ω_1. The unit velocity vector and the orientation of P are used to construct the transformation matrix that rotates the coordinate frame (x, y) into the (x_n, y_n) plane of the navigation frame.

The DCM C_P^n, formed as shown below

$$C_P^n = \left[\begin{array}{c|c|c} \vec{V}_{1n} & \vec{\omega}_{1n} \times \vec{V}_{1n} & \vec{\omega}_{1n} \end{array} \right]$$

transforms vectors resolved in the plane P into vectors resolved in the navigation frame. The range vector $\vec{R}$ resolved in the navigation frame is

$$\vec{R}_n = \left[\begin{array}{c} X_P - X_0 \\ Y_P - Y_0 \\ Z_P - Z_0 \end{array} \right] \tag{3.29}$$

Since,

$$(C_P^n)^T \vec{R}_n = \begin{bmatrix} x \\ y \\ 0 \end{bmatrix}$$

then

$$\vec{R}_n = C_P^n \begin{bmatrix} x \\ y \\ 0 \end{bmatrix} \tag{3.30}$$

3.4.2 Basic Linear Regression. It is apparent from Figure 3.9 that

$$x = R\cos\gamma_D \quad \text{and} \quad y = R\sin\gamma_D \tag{3.31}$$

Realizing that only an estimate of γ_D is available, $\gamma_D = \hat{\gamma}_D + \upsilon_{\gamma_D}$ is substituted into Equation (3.31) to yield

$$\begin{aligned} x &\approx R\cos\hat{\gamma}_D - R\sin\hat{\gamma}_D \cdot \upsilon_{\gamma_D} \\ y &\approx R\sin\hat{\gamma}_D + R\cos\hat{\gamma}_D \cdot \upsilon_{\gamma_D} \end{aligned}$$

The estimation error of γ_D, υ_{γ_D} is modeled as white Gaussian noise with zero mean and represented as $\upsilon_{\gamma_D} = \mathcal{N}(0, \sigma^2_{\gamma_D})$. Using the equalities

$$x = K_x V \quad \text{and} \quad y = K_y V \tag{3.32}$$

derived in Section 2.3.2, Equation (2.18) yields the linear regression in the primary parameters R and V.

$$\begin{bmatrix} V_m \\ 0 \\ 0 \end{bmatrix} = \begin{bmatrix} 0 & 1 \\ \cos\hat{\gamma}_D & -K_x \\ \sin\hat{\gamma}_D & -K_y \end{bmatrix} \begin{bmatrix} R \\ V \end{bmatrix} + \begin{bmatrix} 0 & 1 \\ -R\sin\hat{\gamma}_D & 0 \\ R\cos\hat{\gamma}_D & 0 \end{bmatrix} \begin{bmatrix} \upsilon_{\gamma_D} \\ \upsilon_V \end{bmatrix} \tag{3.33}$$

Equations (3.29), (3.30), (3.31), and (3.32) are used to produce Equation (3.34).

$$\begin{bmatrix} X_P - X_0 \\ Y_P - Y_0 \\ Z_P - Z_0 \end{bmatrix} = RC_P^n \begin{bmatrix} \cos\gamma_D \\ \sin\gamma_D \\ 0 \end{bmatrix} \tag{3.34}$$

Substituting $H = \hat{H} + \upsilon_H$, $\gamma = \hat{\gamma} + \upsilon_\gamma$, and $\gamma_D = \hat{\gamma_D} + \upsilon_{\gamma_D}$ produces the linear regression in the parameter $(R, X_0, Y_0, Z_0, X_P, Y_P, Z_P)$ given in Equation (3.35).

$$\begin{bmatrix} \cos\hat{\gamma}_{\mathrm{D}}\cos\hat{\gamma}\cos\hat{H}-\omega_y\sin\hat{\gamma}\sin\hat{\gamma}_D-\omega_z\cos\hat{\gamma}\sin\hat{H}\sin\hat{\gamma}_D & 1\,0\,0\,-1\,0\,0 \\ \cos\hat{\gamma}\sin\hat{H}\cos\hat{\gamma}_D+\omega_z\cos\hat{\gamma}\cos\hat{H}\sin\hat{\gamma}_D+\omega_x\sin\hat{\gamma}\sin\hat{\gamma}_D & 0\,1\,0\,0\,-1\,0 \\ -\sin\hat{\gamma}\cos\hat{\gamma}_D+\omega_x\cos\hat{\gamma}\sin\hat{H}\sin\hat{\gamma}_D-\omega_y\cos\hat{\gamma}\cos\hat{H}\sin\hat{\gamma}_D & 0\,0\,1\,0\,0\,-1 \end{bmatrix} \begin{bmatrix} R \\ X_0 \\ Y_0 \\ Z_0 \\ X_P \\ Y_P \\ Z_P \end{bmatrix}$$
$$+\hat{R}^- \begin{bmatrix} -\sin\hat{\gamma}_D\cos\hat{\gamma}\cos\hat{H}-\omega_y\sin\hat{\gamma}\cos\hat{\gamma}_D-\omega_z\cos\hat{\gamma}\sin\hat{H}\cos\hat{\gamma}_D, \\ -\cos\hat{\gamma}\sin\hat{H}\sin\hat{\gamma}_D+\omega_z\cos\hat{\gamma}\cos\hat{H}\cos\hat{\gamma}_D+\omega_x\sin\hat{\gamma}\cos\hat{\gamma}_D, \\ \sin\hat{\gamma}\sin\hat{\gamma}_D+\omega_x\cos\hat{\gamma}\sin\hat{H}\cos\hat{\gamma}_D-\omega_y\cos\hat{\gamma}\cos\hat{H}\cos\hat{\gamma}_D, \\ -\cos\hat{\gamma}_D\sin\hat{\gamma}\cos\hat{H}-\omega_y\cos\hat{\gamma}\sin\hat{\gamma}_D+\omega_z\sin\hat{\gamma}\sin\hat{H}\sin\hat{\gamma}_D, \\ -\sin\hat{\gamma}\sin\hat{H}\cos\hat{\gamma}_D-\omega_z\sin\hat{\gamma}\cos\hat{H}\sin\hat{\gamma}_D+\omega_x\cos\hat{\gamma}\sin\hat{\gamma}_D, \\ -\cos\hat{\gamma}\cos\hat{\gamma}_D-\omega_x\sin\hat{\gamma}\sin\hat{H}\sin\hat{\gamma}_D+\omega_y\sin\hat{\gamma}\cos\hat{H}\sin\hat{\gamma}_D, \end{bmatrix}$$
$$\begin{bmatrix} -\cos\hat{\gamma}_D\cos\hat{\gamma}\sin\hat{H}-\omega_z\cos\hat{\gamma}\cos\hat{H}\sin\hat{\gamma}_D \\ \cos\hat{\gamma}\cos\hat{H}\cos\hat{\gamma}_D-\omega_z\cos\hat{\gamma}\sin\hat{H}\sin\hat{\gamma}_D \\ \omega_x\cos\hat{\gamma}\cos\hat{H}\sin\hat{\gamma}_D+\omega_y\cos\hat{\gamma}\sin\hat{H}\sin\hat{\gamma}_D \end{bmatrix} \begin{bmatrix} \upsilon_{\gamma_D} \\ \upsilon_\gamma \\ \upsilon_H \end{bmatrix} = \begin{bmatrix} 0 \\ 0 \\ 0 \end{bmatrix} \tag{3.35}$$

3.4.3 Nonlinear Equality Constraint. The range R satisfies

$$R - \sqrt{(X_P - X_0)^2 + (Y_P - Y_0)^2 + (Z_P - Z_0)^2} = 0 \tag{3.36}$$

Linearization of Equation (3.36) is performed by defining the parameter vector

$$X \triangleq \begin{bmatrix} X_0 & Y_0 & Z_0 & X_P & Y_P & Z_P \end{bmatrix}^T$$

and using the notation

$$f(X) \triangleq \sqrt{(X_P - X_0)^2 + (Y_P - Y_0)^2 + (Z_P - Z_0)^2}$$

so that Equation (3.36)is written as $R - f(X) = 0$. The approximation for $f(X)$ is

$$f(X) = f(\hat{X}^- + X - \hat{X}^-) \approx f(\hat{X}^-) + \nabla f|_{\hat{X}^-}(X - \hat{X}^-) \tag{3.37}$$

where $\hat{X}^-$ is the prior estimate of the parameter X, and $\hat{R}^-$ is the prior estimate of the range R. Inserting Equation (3.37) into Equation (3.36) produces

$$R - \nabla f|_{\hat{X}^-} X = -\nabla f|_{\hat{X}^-} \hat{X}^- + f(\hat{X}^-)$$

The gradient of f

$$\nabla f|_{\hat{X}^-} = \left[\frac{\hat{X}_0^- - \hat{X}_P^-}{\hat{R}^-},\ \frac{\hat{Y}_0^- - \hat{Y}_P^-}{\hat{R}^-},\ \frac{\hat{Z}_0^- - \hat{Z}_P^-}{\hat{R}^-},\ \frac{\hat{X}_P^- - \hat{X}_0^-}{\hat{R}^-},\ \frac{\hat{Y}_P^- - \hat{Y}_0^-}{\hat{R}^-},\ \frac{\hat{Z}_P^- - \hat{Z}_0^-}{\hat{R}^-}\right] \tag{3.38}$$

Inserting Equation (3.38) into Equation (3.37) yields

$$R + \frac{\hat{X}_P^- - \hat{X}_0^-}{\hat{R}^-}X_0 + \frac{\hat{Y}_P^- - \hat{Y}_0^-}{\hat{R}^-}Y_0 + \frac{\hat{Z}_P^- - \hat{Z}_0^-}{\hat{R}^-}Z_0 - \frac{\hat{X}_P^- - \hat{X}_0^-}{\hat{R}^-}X_P - \frac{\hat{Y}_P^- - \hat{Y}_0^-}{\hat{R}^-}Y_P - \frac{\hat{Z}_P^- - \hat{Z}_0^-}{\hat{R}^-}Z_P =$$
$$\frac{\hat{X}_P^- - \hat{X}_0^-}{\hat{R}^-}\hat{X}_0^- + \frac{\hat{Y}_P^- - \hat{Y}_0^-}{\hat{R}^-}\hat{Y}_0^- + \frac{\hat{Z}_P^- - \hat{Z}_0^-}{\hat{R}^-}\hat{Z}_0^- - \frac{\hat{X}_P^- - \hat{X}_0^-}{\hat{R}^-}\hat{X}_P^- - \frac{\hat{Y}_P^- - \hat{Y}_0^-}{\hat{R}^-}\hat{Y}_P^- - \frac{\hat{Z}_P^- - \hat{Z}_0^-}{\hat{R}^-}\hat{Z}_P^- + \hat{R}^-$$

The right hand side of the equation is simplified to

$$-\frac{1}{\hat{R}^-}\left[(\hat{X}_P^- - \hat{X}_0^-)^2 + (\hat{Y}_P^- - \hat{Y}_0^-)^2 + (\hat{Z}_P^- - \hat{Z}_0^-)^2\right] + \hat{R}^- = 0$$

Thus, the additional linear regression equation in the parameter $[R \vdots X]^T$ is obtained

$$\left[1, \frac{\hat{X}_P^- - \hat{X}_0^-}{\hat{R}^-}, \frac{\hat{Y}_P^- - \hat{Y}_0^-}{\hat{R}^-}, \frac{\hat{Z}_P^- - \hat{Z}_0^-}{\hat{R}^-}, -\frac{\hat{X}_P^- - \hat{X}_0^-}{\hat{R}^-}, -\frac{\hat{Y}_P^- - \hat{Y}_0^-}{\hat{R}^-}, -\frac{\hat{Z}_P^- - \hat{Z}_0^-}{\hat{R}^-}\right] \begin{bmatrix} R \\ \cdots \\ X \end{bmatrix} = 0 \tag{3.39}$$

The relationships developed so far are used to compose the linear regression equation used in the INS position estimate updating algorithm.

3.4.4 Stadiametry. The INS provides measurements of the aircraft's positional navigation variables, viz., the velocity V_m, and the aircraft's current position X_{0_m}, Y_{0_m}, and Z_{0_m}. The aircraft's baro-altitude measurement can be used to reduce the error in Z_{0_m}. The INS measurements can also be augmented with prior information on the ground object's position X_{P_m}, Y_{P_m}, and Z_{P_m}. Concerning the range R to the ground object: the measurement can be derived from direct radar ranging, if available. Most importantly, the error in R_m is assumed small, the rational being that R_m is obtained from an application of the Law of Sines to the triangle shown in Figure 3.3. In other words, the critical stadiametric relationship afforded by the optical measurement is used:

$$R_m = \frac{\sin(\gamma_D + \sigma)}{\sin \sigma} V_m t \tag{3.40}$$

where σ is the LOS excursion and t is the duration of the measurement interval.

3.4.5 Linear Regression. Equations (3.33), (3.35), and (3.39) are combined into a linear regression in the parameter

$$(R, V, X_0, Y_0, Z_0, X_P, Y_P, Z_P)^T$$

where also the INS provided measurements and the prior information on the ground object position are included, as shown in Equation (3.41).

$$
\begin{bmatrix}
0 & 1 & 0 & 0 & 0 & 0 & 0 & 0 \\
\cos\hat{\gamma}_D & -K_X & 0 & 0 & 0 & 0 & 0 & 0 \\
\sin\hat{\gamma}_D & -K_Y & 0 & 0 & 0 & 0 & 0 & 0 \\
A_1 & 0 & 1 & 0 & 0 & -1 & 0 & 0 \\
A_2 & 0 & 0 & 1 & 0 & 0 & -1 & 0 \\
A_3 & 0 & 0 & 0 & 1 & 0 & 0 & -1 \\
1 & 0 & \frac{\hat{X}_P^- - \hat{X}_0^-}{\hat{R}^-} & \frac{\hat{Y}_P^- - \hat{Y}_0^-}{\hat{R}^-} & \frac{\hat{Z}_P^- - \hat{Z}_0^-}{\hat{R}^-} & -\frac{\hat{X}_P^- - \hat{X}_0^-}{\hat{R}^-} & -\frac{\hat{Y}_P^- - \hat{Y}_0^-}{\hat{R}^-} & -\frac{\hat{Z}_P^- - \hat{Z}_0^-}{\hat{R}^-} \\
0 & 0 & 1 & 0 & 0 & 0 & 0 & 0 \\
0 & 0 & 0 & 1 & 0 & 0 & 0 & 0 \\
0 & 0 & 0 & 0 & 1 & 0 & 0 & 0 \\
0 & 0 & 0 & 0 & 0 & 1 & 0 & 0 \\
0 & 0 & 0 & 0 & 0 & 0 & 1 & 0 \\
0 & 0 & 0 & 0 & 0 & 0 & 0 & 1 \\
1 & 0 & 0 & 0 & 0 & 0 & 0 & 0
\end{bmatrix}
\begin{bmatrix} R \\ V \\ X_0 \\ Y_0 \\ Z_0 \\ X_P \\ Y_P \\ Z_P \end{bmatrix}
+
\begin{bmatrix}
0 & 1 & 0 & 0 & 0 & 0 & 0 & 0 & 0 & 0 \\
-\hat{R}^- \sin\hat{\gamma}_D & 0 & 0 & 0 & 0 & 0 & 0 & 0 & 0 & 0 \\
\hat{R}^- \cos\hat{\gamma}_D & 0 & 0 & 0 & 0 & 0 & 0 & 0 & 0 & 0 \\
B_1 & 0 & C_1 & D_1 & 0 & 0 & 0 & 0 & 0 & 0 \\
B_2 & 0 & C_2 & D_2 & 0 & 0 & 0 & 0 & 0 & 0 \\
B_3 & 0 & C_3 & D_3 & 0 & 0 & 0 & 0 & 0 & 0 \\
0 & 0 & 0 & 0 & 0 & 0 & 0 & 0 & 0 & 0 \\
0 & 0 & 0 & 0 & 1 & 0 & 0 & 0 & 0 & 0 \\
0 & 0 & 0 & 0 & 0 & 1 & 0 & 0 & 0 & 0 \\
0 & 0 & 0 & 0 & 0 & 0 & 1 & 0 & 0 & 0 \\
0 & 0 & 0 & 0 & 0 & 0 & 0 & 1 & 0 & 0 \\
0 & 0 & 0 & 0 & 0 & 0 & 0 & 0 & 1 & 0 \\
0 & 0 & 0 & 0 & 0 & 0 & 0 & 0 & 0 & 1
\end{bmatrix}
\begin{bmatrix} \upsilon_{\gamma_D} \\ \upsilon_V \\ \upsilon_\gamma \\ \upsilon_H \\ \upsilon_{X_0} \\ \upsilon_{Y_0} \\ \upsilon_{Z_0} \\ \upsilon_{X_P} \\ \upsilon_{Y_P} \\ \upsilon_{Z_P} \\ \upsilon_R \end{bmatrix}
=
\begin{bmatrix} V_m \\ 0 \\ 0 \\ 0 \\ 0 \\ 0 \\ X_{0_m} \\ Y_{0_m} \\ Z_{0_m} \\ X_{P_m} \\ Y_{P_m} \\ Z_{P_m} \\ R_m \end{bmatrix}
\tag{3.41}
$$

where, in vector notation,

$$
A = \begin{bmatrix} \cos\hat{\gamma}_{\mathrm{D}} \cos\hat{\gamma} \cos\hat{H} - \omega_y \sin\hat{\gamma} \sin\hat{\gamma}_D - \omega_z \cos\hat{\gamma} \sin\hat{H} \sin\hat{\gamma}_D \\ \cos\hat{\gamma} \sin\hat{H} \cos\hat{\gamma}_D + \omega_z \cos\hat{\gamma} \cos\hat{H} \sin\hat{\gamma}_D + \omega_x \sin\hat{\gamma} \sin\hat{\gamma}_D \\ -\sin\hat{\gamma} \cos\hat{\gamma}_D + \omega_x \cos\hat{\gamma} \sin\hat{H} \sin\hat{\gamma}_D - \omega_y \cos\hat{\gamma} \cos\hat{H} \sin\hat{\gamma}_D \end{bmatrix}
$$

$$
B = \hat{R}^- \begin{bmatrix} -\sin\hat{\gamma}_D \cos\hat{\gamma} \cos\hat{H} - \omega_y \sin\hat{\gamma} \cos\hat{\gamma}_D - \omega_z \cos\hat{\gamma} \sin\hat{H} \cos\hat{\gamma}_D \\ -\cos\hat{\gamma} \sin\hat{H} \sin\hat{\gamma}_D + \omega_z \cos\hat{\gamma} \cos\hat{H} \cos\hat{\gamma}_D + \omega_x \sin\hat{\gamma} \cos\hat{\gamma}_D \\ \sin\hat{\gamma} \sin\hat{\gamma}_D + \omega_x \cos\hat{\gamma} \sin\hat{H} \cos\hat{\gamma}_D - \omega_y \cos\hat{\gamma} \cos\hat{H} \cos\hat{\gamma}_D \end{bmatrix}
$$

$$
C = \hat{R}^- \begin{bmatrix} -\cos\hat{\gamma}_D \sin\hat{\gamma} \cos\hat{H} - \omega_y \cos\hat{\gamma} \sin\hat{\gamma}_D + \omega_z \sin\hat{\gamma} \sin\hat{H} \sin\hat{\gamma}_D \\ -\sin\hat{\gamma} \sin\hat{H} \cos\hat{\gamma}_D - \omega_z \sin\hat{\gamma} \cos\hat{H} \sin\hat{\gamma}_D + \omega_x \cos\hat{\gamma} \sin\hat{\gamma}_D \\ -\cos\hat{\gamma} \cos\hat{\gamma}_D - \omega_x \sin\hat{\gamma} \sin\hat{H} \sin\hat{\gamma}_D + \omega_y \sin\hat{\gamma} \cos\hat{H} \sin\hat{\gamma}_D \end{bmatrix}
$$

$$
D = \hat{R}^- \begin{bmatrix} -\cos\hat{\gamma}_D \cos\hat{\gamma} \sin\hat{H} - \omega_z \cos\hat{\gamma} \cos\hat{H} \sin\hat{\gamma}_D \\ \cos\hat{\gamma} \cos\hat{H} \cos\hat{\gamma}_D - \omega_z \cos\hat{\gamma} \sin\hat{H} \sin\hat{\gamma}_D \\ \omega_x \cos\hat{\gamma} \cos\hat{H} \sin\hat{\gamma}_D + \omega_y \cos\hat{\gamma} \sin\hat{H} \sin\hat{\gamma}_D \end{bmatrix}
$$

The linear regression Equation (3.41) is in the form

$$
Z = HX + \Gamma V
$$

where Z represents the 14×1 measurement vector, H represents the 14×8 regressor matrix, Γ represents the 14×11 measurement noise input matrix, and V represents the 11×1 measurement noise vector. Assuming the measurement noise components are not correlated, the 14×14 equation error covariance matrix is

$$R_{noise} = \Gamma \begin{bmatrix} \sigma^2_{\gamma_D} & 0 & 0 & 0 & 0 & 0 & 0 & 0 & 0 & 0 & 0 \\ 0 & \sigma^2_V & 0 & 0 & 0 & 0 & 0 & 0 & 0 & 0 & 0 \\ 0 & 0 & \sigma^2_\gamma & 0 & 0 & 0 & 0 & 0 & 0 & 0 & 0 \\ 0 & 0 & 0 & \sigma^2_H & 0 & 0 & 0 & 0 & 0 & 0 & 0 \\ 0 & 0 & 0 & 0 & \sigma^2_{X_0} & 0 & 0 & 0 & 0 & 0 & 0 \\ 0 & 0 & 0 & 0 & 0 & \sigma^2_{Y_0} & 0 & 0 & 0 & 0 & 0 \\ 0 & 0 & 0 & 0 & 0 & 0 & \sigma^2_{Z_0} & 0 & 0 & 0 & 0 \\ 0 & 0 & 0 & 0 & 0 & 0 & 0 & \sigma^2_{X_P} & 0 & 0 & 0 \\ 0 & 0 & 0 & 0 & 0 & 0 & 0 & 0 & \sigma^2_{Y_P} & 0 & 0 \\ 0 & 0 & 0 & 0 & 0 & 0 & 0 & 0 & 0 & \sigma^2_{Z_P} & 0 \\ 0 & 0 & 0 & 0 & 0 & 0 & 0 & 0 & 0 & 0 & \sigma^2_R \end{bmatrix} \Gamma^T$$

The measurement noise components are modeled as white Gaussian noise with zero mean.

The linear regression (3.41) would normally be solved using the Minimum Variance formulae (3.28) where $\hat{X}^+$ is the minimum variance parameter estimate and P^+ is the predicted parameter estimation error covariance matrix. $\hat{X}^+$ provides the updated estimate of the aircraft's position and velocity, and also the position of the unknown ground object. The updating of the initial aircraft position, the aircraft velocity, and the geo-location of the stationary ground object jointly occur at the completion of the bearings measurement sequence, at time T, of which time the INS aiding task is accomplished.

3.4.6 Linear Regression Solution. Calculating $\hat{X}^+$ and P^+ using Equation (3.28) would be straight forward; however, Equation (3.41) contains the matrix R_{noise} which is rank deficient and thus cannot be inverted. Indeed, the rank of R_{noise} is equal to the rank of Γ which is 11, and thus the rank deficiency of the matrix R_{noise} is three. Careful mathematical analysis is required to produce a solution to the non-conventional, singular, linear regression in Equation (3.41).

Consider the singular linear regression in the standard form

$$Z = HX + \Gamma V \tag{3.42}$$

where the parameter vector $X \in \Re^n$, the measurement vector $Z \in \Re^N$, the regressor matrix H is $N \times n$ with rank n, Γ is a full rank $N \times m$ noise input matrix, and the random noise vector $V \in \Re^m$ with zero mean, Gaussian statistics. The rank deficiency of the equation error covariance matrix R_{noise} is $n - m$.

A Singular Value Decomposition of the positive, semi-definite real symmetric matrix R_{noise} is performed and produces $R_{noise} = TST^T$. T is an $N \times N$ orthonormal matrix and S is a diagonal matrix of the form

$$S = \begin{bmatrix} D & \vdots & 0 \\ \cdots & & \cdots \\ 0 & \vdots & 0 \end{bmatrix}$$

where D is an invertible diagonal $m \times m$ sub-matrix of S. R_{noise} is equivalent to

$$R_{noise} = T \begin{bmatrix} \sqrt{D} & \vdots & 0 \\ \cdots & & \cdots \\ 0 & \vdots & 0 \end{bmatrix} \begin{bmatrix} \sqrt{D} & \vdots & 0 \\ \cdots & & \cdots \\ 0 & \vdots & 0 \end{bmatrix} T^T$$

Multiply Equation (3.42) from the left by the matrix

$$\begin{bmatrix} D^{-\frac{1}{2}} & \vdots & 0 \\ \cdots & & \cdots \\ 0 & \vdots & I_{N-m} \end{bmatrix} T^T$$

to obtain Equation (3.43)

$$\begin{bmatrix} D^{-\frac{1}{2}} & \vdots & 0 \\ \cdots & & \cdots \\ 0 & \vdots & I_{N-m} \end{bmatrix} T^T Z = \begin{bmatrix} D^{-\frac{1}{2}} & \vdots & 0 \\ \cdots & & \cdots \\ 0 & \vdots & I_{N-m} \end{bmatrix} T^T H X + W \tag{3.43}$$

where the Gaussian random noise vector W is defined as

$$W = \begin{bmatrix} D^{-\frac{1}{2}} & \vdots & 0 \\ \cdots & & \cdots \\ 0 & \vdots & I_{N-m} \end{bmatrix} T^T \Gamma V$$

The following relationship is established:

$$\begin{aligned} E\left\{WW^T\right\} &= \begin{bmatrix} D^{-\frac{1}{2}} & \vdots & 0 \\ \cdots & & \cdots \\ 0 & \vdots & I_{N-m} \end{bmatrix} T^T E\left\{\Gamma V V^T \Gamma^T\right\} T \begin{bmatrix} D^{-\frac{1}{2}} & \vdots & 0 \\ \cdots & & \cdots \\ 0 & \vdots & I_{N-m} \end{bmatrix} \\ &= \begin{bmatrix} D^{-\frac{1}{2}} & \vdots & 0 \\ \cdots & & \cdots \\ 0 & \vdots & I_{N-m} \end{bmatrix} T^T R T \begin{bmatrix} D^{-\frac{1}{2}} & \vdots & 0 \\ \cdots & & \cdots \\ 0 & \vdots & I_{N-m} \end{bmatrix} \\ &= \begin{bmatrix} D^{-\frac{1}{2}} & \vdots & 0 \\ \cdots & & \cdots \\ 0 & \vdots & I_{N-m} \end{bmatrix} T^T T \begin{bmatrix} D^{\frac{1}{2}} & \vdots & 0 \\ \cdots & & \cdots \\ 0 & \vdots & 0 \end{bmatrix} \begin{bmatrix} D^{\frac{1}{2}} & \vdots & 0 \\ \cdots & & \cdots \\ 0 & \vdots & 0 \end{bmatrix} T^T T \begin{bmatrix} D^{-\frac{1}{2}} & \vdots & 0 \\ \cdots & & \cdots \\ 0 & \vdots & I_{N-m} \end{bmatrix} \\ &= \begin{bmatrix} D^{-\frac{1}{2}} & \vdots & 0 \\ \cdots & & \cdots \\ 0 & \vdots & I_{N-m} \end{bmatrix} \begin{bmatrix} D & \vdots & 0 \\ \cdots & & \cdots \\ 0 & \vdots & 0 \end{bmatrix} \begin{bmatrix} D^{-\frac{1}{2}} & \vdots & 0 \\ \cdots & & \cdots \\ 0 & \vdots & I_{N-m} \end{bmatrix} \\ &= \begin{bmatrix} I_m & \vdots & 0 \\ \cdots & & \cdots \\ 0 & \vdots & 0 \end{bmatrix} \end{aligned} \tag{3.44}$$

Equation (3.44) proves that

$$E\{WW^T\} = \begin{bmatrix} I_m & \vdots & 0 \\ \cdots & & \cdots \\ 0 & \vdots & 0 \end{bmatrix} \tag{3.45}$$

Thus W is partitioned as $W = \left[\begin{array}{c|c} w_1 & 0 \end{array} \right]^T$ where $w_1 \in \Re^m$ and $w_1 = \mathcal{N}(0, I_m)$.

Define the partitioned vector

$$T^T Z = \left[\begin{array}{c} z_1 \\ \cdots \\ z_2 \end{array} \right]$$

and the partitioned matrix

$$T^T H = \left[\begin{array}{c} H_1 \\ \cdots \\ H_2 \end{array} \right]$$

with $z_1 \in \Re^m$ and H_1 a $m \times n$ matrix, and $z_2 \in \Re^{N-m}$ and H_2 a $(N-m) \times n$ matrix. This yields a reduced order non-singular standard linear regression in the form $D^{-1/2} z_1 = D^{-1/2} H_1 X + w_1$ and a set of $N - m$ linear equality constraints in the form $z_2 = H_2 X$.

The matrix H_2 is further partitioned into H_{21} and H_{22} as follows:

$$H_2 = \left[\begin{array}{c|c} H_{21} & H_{22} \end{array} \right]$$

where H_{22} is a non-singular $(N-m) \times (N-m)$ matrix. H_1 is also partitioned into two separate matrices H_{11} and H_{12} as follows:

$$H_1 = \left[\begin{array}{c|c} H_{11} & H_{12} \end{array} \right]$$

where H_{12} is a $m \times (N-m)$ matrix. The parameter vector X is partitioned into X_1 and X_2 as follows:

$$X = \left[\begin{array}{c} X_1 \\ \cdots \\ X_2 \end{array} \right]$$

where $X_2 \in \Re^{N-m}$. Using the partitions of z, X, H_1, and H_2, the linear regression equation is rewritten as

$$z_2 = H_{21}X_1 + H_{22}X_2 \tag{3.46}$$

and

$$z_1 = H_{11}X_1 + H_{12}X_2 + D^{\frac{1}{2}}w_1 \tag{3.47}$$

Solving Equation (3.46) for X_2 yields

$$X_2 = H_{22}^{-1}z_2 - H_{22}^{-1}H_{21}X_1 \tag{3.48}$$

Substituting Equation (3.48) into Equation (3.47) yields the reduced linear regression

$$z_1 - H_{12}H_{22}^{-1}z_2 = (H_{11} - H_{12}H_{22}^{-1}H_{21})X_1 + D^{\frac{1}{2}}w_1 \tag{3.49}$$

where

$$R = E\left\{D^{\frac{1}{2}}w_1w_1^TD^{\frac{1}{2}}\right\} = D$$

The linear regression Equation (3.49) is solved using the Minimum Variance formulae (3.28), where $Z = z_1 - H_{12}H_{22}^{-1}z_2$, $H = H_{11} - H_{12}H_{22}^{-1}H_{21}$, $X = X_1$, and $V = D^{1/2}w_1$. This yields Equations (3.50) and (3.51).

$$P_{X_1} = \left[(H_{11} - H_{12}H_{22}^{-1}H_{21})^TD^{-1}(H_{11} - H_{12}H_{22}^{-1}H_{21})\right]^{-1} \tag{3.50}$$

$$\hat{X}_1 = P_{X_1}(H_{11} - H_{12}H_{22}^{-1}H_{21})^TD^{-1}(z_1 - H_{12}H_{22}^{-1}z_2) \tag{3.51}$$

Substituting the estimated parameter $\hat{X}_1$ into Equation (3.48) produces an estimate of the parameter $\hat{X}_2$ in the form

$$\hat{X}_2 = H_{22}^{-1}z_2 - H_{22}^{-1}H_{21}\hat{X}_1 \tag{3.52}$$

where

$$P_{X_2} = H_{22}^{-1} H_{21} P_{X_1} H_{21}^T (H_{22}^{-1})^T \tag{3.53}$$

The solution of the linear regression produces $\hat{X}_1$, $\hat{X}_2$, P_{X_1}, and P_{X_2}. The parameters $\hat{X}$ and P_X are defined as

$$\hat{X} = \begin{bmatrix} \hat{X}_1 \\ \cdots \\ \hat{X}_2 \end{bmatrix}$$

and

$$P_X = \begin{bmatrix} P_{X_1} & \vdots & 0 \\ \cdots & & \cdots \\ 0 & \vdots & P_{X_2} \end{bmatrix}$$

respectively.

3.5 Summary

This chapter provides the aiding algorithm which makes INS aiding using passive, bearings-only measurements of an unknown ground object possible. The heart of the algorithm lies in the linearization of Equation (3.36) which shows the geometric relationship between the LOS range, the initial position of the aircraft, and the position of the unknown ground object. Equation (3.41) must be carefully partitioned to produce an invertible error covariance matrix for use in the Minimum Variance formulae to produce the best estimate of the desired parameters.

IV. Simulation Results and Analysis

The novel INS aiding method using passive, bearings-only measurements of an unknown, but stationary, ground object over time is validated in simulation experiments. MatLab® simulations are used to test and validate the aiding algorithm, and also determine which flight profiles are best for INS aiding using bearings-only measurements.

4.1 Methodology

The simulation begins with the selection of a scenario. A set of initial conditions is chosen to generate the true flight profile of the aircraft as well as the true bearings measurements. The latter are then corrupted with measurement noise. The INS measurements are simulated using the true initial position and velocity values, to which random errors generated from a zero-mean normal distribution are added to simulate the INS errors at the initial point of the measurement interval. The drift of the INS during the measurement interval is of no concern because the only information used by the aiding algorithm comes from the INS at the initial measurement point. The variance of the normal distribution of the INS provided position and velocity is dependent on the quality of the INS modeled in the simulation. The INS measurements are then used in the linear regression algorithm to produce a new estimate of the position and velocity of the aircraft as well as an estimate of the unknown ground object's location. Since linearization is employed, iterations are required. The algorithm converges quickly, within two or three iterations; therefore, the total number of iterations does not need to be set very high. This process is run through a set number of Monte Carlo evaluations with the same INS errors but different bearings measurement errors. This constitutes a single Monte Carlo run in itself and is repeated for different INS measurement errors. The simulation setup is summarized in Figure 4.1.

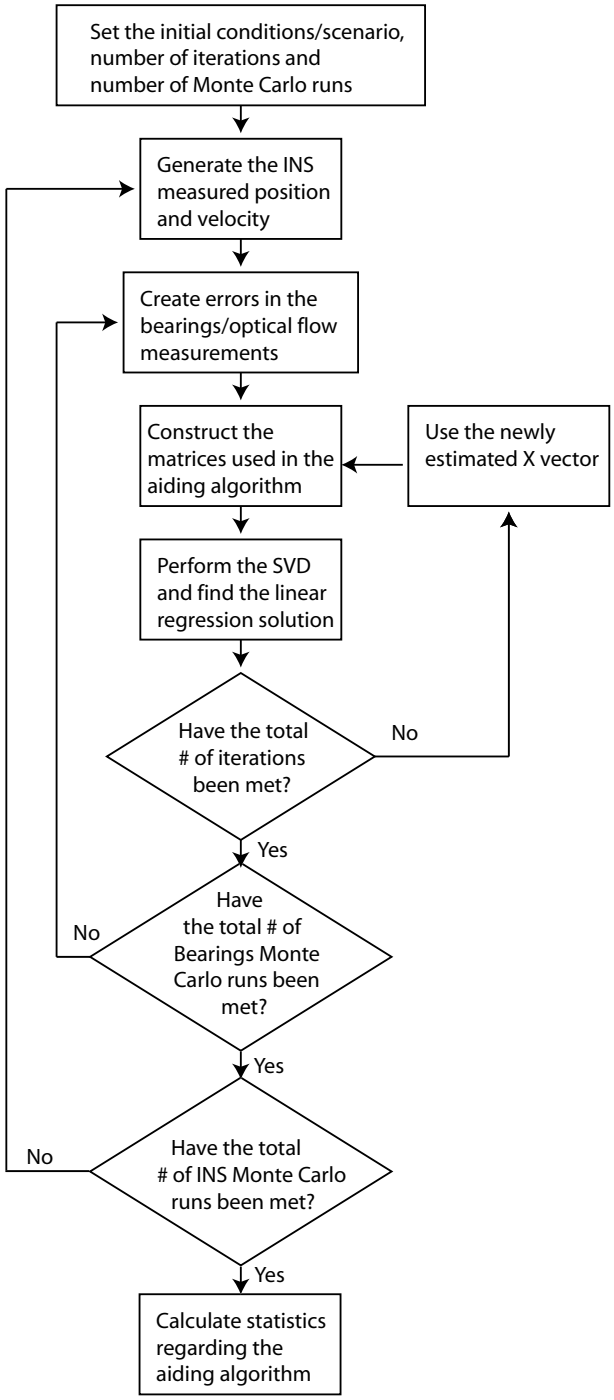

Figure 4.1 Simulation Flow Chart

4.2 Flight Profile Generation

The flight profile renders the path and velocity the aircraft traverses through three-dimensional space as the stationary ground object is tracked. The flight profile also contains σ measurements from the tracking system as well as the unit LOS vector and the LOS range. The flight profile is generated using the aircraft's initial position, the location of the ground object that the aircraft is tracking, the number of, and time interval between, the bearings-only measurements, heading, velocity, and flight path angle of the aircraft.

The initial aircraft position and unknown ground object position are expressed in Cartesian coordinate axes as defined in MatLab® according to Figure 4.2. This reference frame is known as the inertial frame. The heading and flight path angle

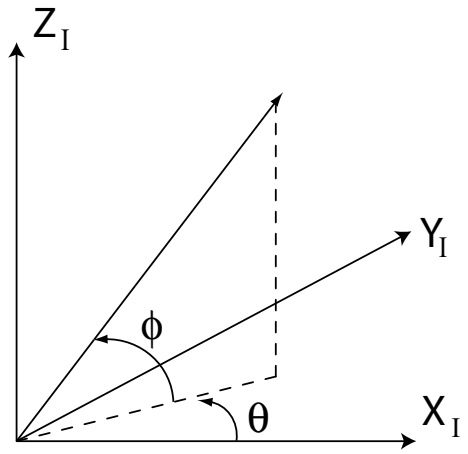

Figure 4.2 Inertial Coordinate Frame

are also expressed in an inertial frame via the angles θ and ϕ. Expressing the initial condition with respect to the inertial frame simplifies plotting and analysis. The aiding algorithm requires the velocity, heading, and flight path angle of the aircraft to be defined with respect to the navigation frame; therefore, the initial conditions are transformed into vectors resolved in the navigation frame. Figure 4.3 is an example plot of a flight profile in MatLab®. The data points along the flight path correspond to when a single bearings-only measurement is recorded. The dashed lines represent

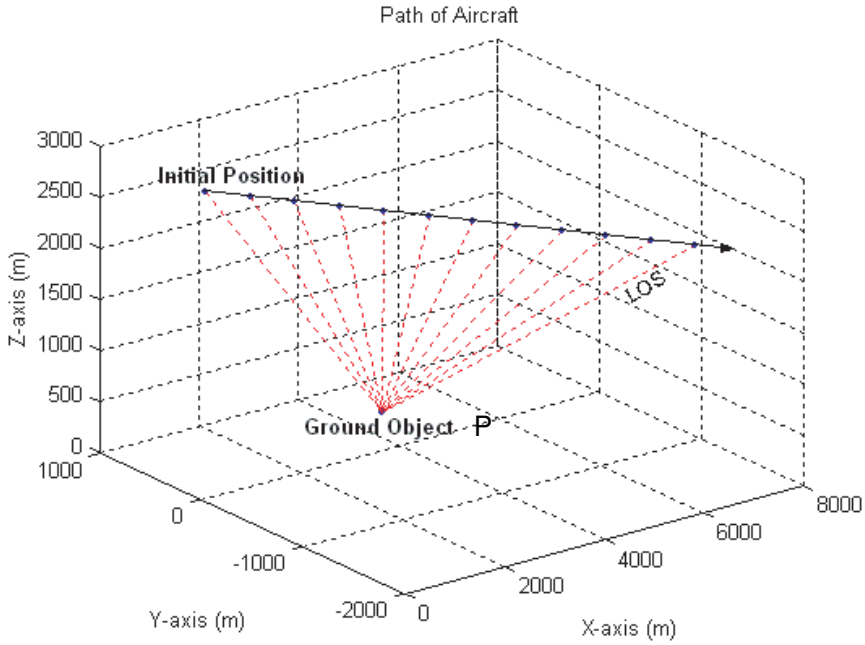

Figure 4.3 Flight Profile Plot

the LOS to the unknown, stationary ground object, which is represented by a single point P in space.

The bearings measurements generated from the flight profile are used to calculate the true angle γ_D between the inertial velocity vector of the aircraft and the initial LOS. This is accomplished through the same process used in the two-dimensional scenario shown in [7] and discussed in Section 2.3.2. Producing noise-corrupted estimates of γ_D is accomplished by adding zero mean Gaussian noise to the true σ measurements.

The MatLab® flight profile function is used to generate and plot the aircraft's true flight path, the INS-measured flight path, and the INS-aided flight path. The INS-measured flight path is generated from noise-corrupted measurements of the initial position, velocity, heading, and flight path angle, as well as the estimated ground object coordinate. The estimated ground object coordinate is calculated using the Law of Sines as described in Section 3.5. The angles $\hat{\gamma}_D$ and $\hat{\sigma}_1$ are used in

conjunction with the estimated distance between the first and second measurement intervals to produce an estimate of the initial LOS range. The estimated initial LOS range ($\hat{R}$), initial unit LOS vector measurement ($\overrightarrow{LOS}_{1b}$), and the INS-measured initial position (X_{0_m}, Y_{0_m}, Z_{0_m}) are used to produce the estimated ground object position (X_{P_m}, Y_{P_m}, Z_{P_m}).

4.3 The INS Aiding Algorithm

The simulation software takes the initial conditions and generates the true and INS-estimated flight profiles as well as the bearings measurements and an estimate of γ_D. The measurements and parameter estimates from the first part of the simulation are used in Equation (3.41) to aid the INS measurements through the Minimum Variance formulae given by Equation (3.28). The simulation calculates the estimated parameter $\hat{X}$ and its estimation error covariance P_X exactly as outlined in Section 3.4. The linear regression solution is iterated a set number of times to demonstrate the convergent properties of the solution. The same initial conditions and INS measurements are used in every Monte Carlo run. The only values that change are the errors in the bearings-only measurements.

The aiding concept is envisioned as a batch process. Once the entire bearings measurement record is obtained, the aiding algorithm is applied and a more accurate estimate of the initial aircraft position, velocity, and ground object location is determined. The estimates are used to calculate a future INS position update time. The aircraft's estimated heading, flight path angle, and velocity are used in conjunction with the aircraft's estimated initial position to produce a more accurate flight profile. For as long as the aircraft maintains its velocity, heading, and flight path angle, future INS aiding positions are created ahead of the aircraft. The INS is then updated at that predetermined position with a new, more accurate estimate of position and velocity - see, e.g., Figure 4.4.

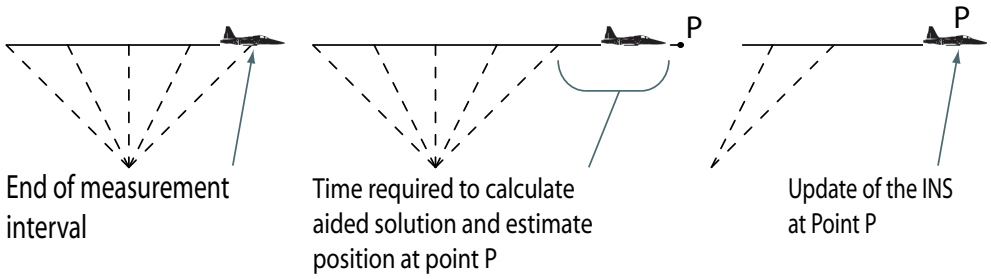

Figure 4.4 INS Aiding Principle

In this work it is assumed that the aircraft maintains its original heading and flight path without any deviations in course or velocity. These restrictions do limit when the aiding algorithm can be applied, but not to a degree in which the aiding concept becomes useless. The measurement interval for INS aiding is often less than one minute, and, operationally at low altitudes, under ten seconds, and requires only four measurements to produce a solution. It is by no means too restrictive to have a pilot/autopilot fly an aircraft along a strait path while maintaining constant velocity for a short period of time. This is especially true if the aircraft's passive sensors are gathering information as part of the mission requirements. Indeed, similar flight restrictions apply during INS transfer alignment and/or when tracking tasks are performed, for example, during a bombing run. A steady wind is not an impediment to the INS update run. A steady wind is seen as an error in the heading and flight path angle of the aircraft; however, heavy turbulence could greatly degrade the accuracy of the optical flow measurement.

4.4 Scenarios

The very nature of this research yields a very large number of interesting INS aiding scenarios. However, only a few important scenarios that provide good insight into INS aiding using passive, bearings-only measurements over time, are covered in this section. The key areas of interest are:

1. The impact of bearings only measurements on a tactical-grade INS.

2. The impact of bearings-only measurements on a tactical-grade INS given prior information.

3. The impact of bearings-only measurements on INS aiding during low/high altitude flight.

Each scenario is repeated a number of times with varying initial positions, unknown ground object locations, velocities, flight path angles, headings, time t between measurements, and total N number of measurements taken. The only common parameters in the various scenarios and in each of the runs that comprise those scenarios are the total number or iterations, the total number of Monte Carlo runs, and the measurement noise corrupting the bearings-only measurements. The maximum number of iterations is set to 10. When the aiding algorithm produces good parameter estimates, it does so within two or three iterations. If the aiding algorithm cannot produce good estimates of the parameters within two or three iterations, it will often oscillate between two poor parameter estimates or diverge. The total number of Monte Carlo runs is set to 100 for the INS measurements and 100 for the bearings measurement. This is equivalent to 10,000 runs for a single engagement. The noise corrupting the bearings measurements (σ) is modeled as a normal distribution denoted as $\mathcal{N}(0, \sigma^2_{\sigma_N})$ where σ_{σ_N} = 5e-4 rad. These are the same values used for the two-dimensional case in [6], [7].

4.5 Statistics

Once each scenario is simulated in the computer, the following statistics are considered:

1. The experimentally obtained mean error (bias) in the parameter estimate.

2. The experimentally obtained standard deviation of the parameter estimate.

3. The predicted standard deviation of the parameter estimate.

4. The probability that the experimentally obtained parameter estimate is within one standard deviation of the predicted parameter estimate.

The bias in the parameter estimate $\hat{X}^+$ is

$$\bar{e}_{\hat{X}^+} = \frac{1}{N_{MC}} \sum_{i=1}^{N_{MC}} (\hat{X}_i^+ - X) \tag{4.1}$$

where $\hat{X}_i^+$ is the parameter estimate in the ith Monte Carlo run, X is the true parameter, and N_{MC} is the total number of Monte Carlo runs in the simulation. A superscript - indicates a value determined at a time before the measurement incorporation, while the superscript + indicates the same value after the measurement incorporation [4]. The experimentally obtained standard deviation of the parameter estimate is equivalent to

$$\hat{\sigma}_{E_X}^+ = \sqrt{\text{rms}_{E_X}^2 - \text{bias}_{E_X}^2} \tag{4.2}$$

where the root mean squared (rms) of the parameter is equal to

$$\text{rms}_{E_X} = \sqrt{\frac{\sum_{i=1}^{N_{MC}} (\hat{X}_i^+ - X)^2}{N_{MC} - 1}}$$

The predicted standard deviation of the parameter estimate is

$$\hat{\sigma}_X^+ = \begin{bmatrix} \sqrt{P_{11}} & 0 & 0 \\ 0 & \ddots & 0 \\ 0 & 0 & \sqrt{P_{NN}} \end{bmatrix} \tag{4.3}$$

The probability that the experimentally obtained parameter estimate is within one standard deviation of the predicted parameter estimate is

$$P_{E_{1-\sigma}} = \frac{\text{Number of times} \left(\left| \hat{X}_i^+ - X \right| \leq \hat{\sigma}_\theta^+ \right)}{N_{MC}} \tag{4.4}$$

$P_{E_{1-\sigma}}$ is a good indication as to how much confidence one should have in the aiding algorithm. Low $P_{E_{1-\sigma}}$ values indicate that the algorithm is not performing as expected and less faith should be placed in the estimated parameter $\hat{X}$. These statistics provide the necessary information to make an informed decision on the feasibility of INS aiding using passive, bearings-only measurements of an unknown ground object.

4.6 Simulation Results

4.6.1 Angular Navigation Variables Update. The update of the angular navigation variables is only examined for the two-dimensional scenarios [7] which entail overflight of the ground object. Table 4.1 shows the results for several flight paths flown during INS aiding runs at a medium altitude of 10,000 feet. The results

Table 4.1 Statistics of γ and θ

Mach/γ [deg]	$\bar{e}_{\hat{\theta}^+}[\mu\text{rad}]$	$\hat{\sigma}^+_{E_\theta}$[mrad]	$\hat{\sigma}^+_{\theta}$[mrad]	$P_{E_{1-\sigma}}$
0.5/-20	24.4319	2.14255	2.12791	39.6
0.8/-20	186.681	2.08650	2.04848	41.4
0.8/-10	24.4338	2.11096	2.12371	40.4
Mach/γ [deg]	$\bar{e}_{\hat{\gamma}^+}[\mu\text{rad}]$	$\hat{\sigma}^+_{E_\gamma}$[mrad]	$\hat{\sigma}^+_{\gamma}$[mrad]	$P_{E_{1-\sigma}}$
0.5/-20	102.944	2.10306	2.12791	39.6
0.8/-20	35.1121	1.95191	2.04848	41.4
0.8/-10	16.7998	2.07291	2.12371	40.4

from Table 4.1 show that the angular navigation variables can be effectively updated using optical flow to enhance the attitude and flight path angle of the aircraft. More Results are documented in [7].

4.6.2 Tactical-Grade INS. A tactical-grade INS is a navigation system often used on platforms which have a very short operation time, for example, munitions. A tactical-grade INS is considerably less expensive than the accurate navigation-grade INS used in aircraft, but at the cost of accuracy. The maximum drift rate of a navigation-grade INS is typically one nautical mile (1852 meters) per hour, whereas the typical maximum drift rate of a tactical-grade INS is one geodetic degree (60

nautical miles) per hour. The tactical-grade INS is chosen over the navigation-grade INS because, without aiding, the tactical-grade INS begins to drift quickly, producing large errors in the navigation solution in only a short period of time. This allows for a greater range of error in the INS to test the aiding algorithm. Successful aiding of a tactical-grade INS guarantees successful aiding of a navigation-grade INS.

Table 4.2 shows the parameters of the three simulations that were run for the first scenario. The initial position of the aircraft and the position of the unknown

Table 4.2 Scenario Parameters

	Sim 1	Sim 2	Sim 3
$V[m/s]$	275	275	275
$\gamma[deg]$	-5	-5	0
$H[deg]$	15	15	0
$X_0[m]$	0	0	0
$Y_0[m]$	0	0	0
$Z_0[m]$	5000	5000	5000
$X_P[m]$	8000	8000	8000
$Y_P[m]$	500	500	0
$Z_P[m]$	200	200	200
$t[s]$	4	4	4
N	12	12	12

ground object are represented in the inertial reference frame and measured in meters. The flight path angle and the heading are also represented in the inertial frame and measured in degrees. The aircraft's velocity is measured in meters per second. The parameter t denotes the time in seconds between measurements and N denotes the total number of measurements taken. Table 4.3 shows the INS measurement errors for each of the simulations. The errors are modeled as normal distributions with zero mean. The standard deviation of each simulation is based on a tactical-grade INS that has been unaided for a short period of time. Simulations 1 and 2 have the same flight parameters but differing degrees of INS error. Simulation 3 examines an over-fly of the ground object, with the same INS errors as in Simulation 1.

Table 4.3 INS Errors - $\mathcal{N}(0, \sigma_N^2)$

	$1-\sigma$	$1-\sigma$	$1-\sigma$
$V[m/s]$	2.5	2.5	2.5
$\gamma[deg]$	1e-4	1e-4	1e-4
$H[deg]$	1e-4	1e-4	1e-4
$X_0[m]$	1850	150	1850
$Y_0[m]$	1850	150	1850
$Z_0[m]$	1850	150	1850

Table 4.4 shows the statistics for all the Monte Carlo runs in the first simulation. This yields the bias in the estimated parameter. Table 4.5 shows the statistics for a single INS Monte Carlo run from the first simulation. The single INS Monte Carlo run gives a better indication of the true performance of the aiding algorithm. It reflects the random nature of the INS error during flight as would be seen in an actual navigation system. For most applications, a single Monte Carlo run is not sufficient to generate reliable statistics; however, in this research, a single INS Monte Carlo run is comprised of 100 measurement Monte Carlo runs, thus producing reliable statistics. The single INS Monte Carlo run is selected at random from the 100 INS Monte Carlo runs. INS_{err} is the error in the INS measured parameters, and $\hat{X}_{err}$ is the error in the estimated parameters provided by the update algorithm. Tables 4.6 and 4.8 show the average statistics for all the Monte Carlo runs in the second and third simulations respectively. Tables 4.7 and 4.9 show the statistics for a single Monte Carlo run from the second and third simulations respectively.

Table 4.4 Simulation 1 Statistics Averaged For All 100 INS Runs

Sim 1	$\bar{e}_{\hat{X}^+}$	$\hat{\sigma}^+_{E_X}$	$\hat{\sigma}^+_X$	$P_{E_{1-\sigma}}$	INS_{err}	$\hat{X}_{err}$
$R[m]$	9.5186	82.0755	73.8843	0.5632	5.7286	9.5186
$V[m/s]$	0.2591	1.9606	2.1745	0.6484	0.2655	0.2591
$X_0[m]$	-196.7971	1681.5984	1308.5299	0.4687	-196.8864	-196.7971
$Y_0[m]$	-183.1617	1371.8616	1308.1491	0.5505	-183.3251	-183.1617
$Z_0[m]$	70.2385	1377.2635	1308.2855	0.5935	69.6635	70.2385
$X_P[m]$	-189.3307	1683.4349	1308.5299	0.4684	-191.9813	-189.3307
$Y_P[m]$	-183.0107	1371.3926	1308.1491	0.5496	-183.0185	-183.0107
$Z_P[m]$	64.5014	1383.0812	1308.2855	0.5807	66.7204	64.5014

Table 4.5 Simulation 1 Statistics For One Run

Sim 1	$\bar{e}_{\hat{X}^+}$	$\hat{\sigma}^+_{E_X}$	$\hat{\sigma}^+_X$	$P_{E_{1-\sigma}}$	INS_{err}	$\hat{X}_{err}$
$R[m]$	27.5210	52.7584	73.8807	0.8300	53.3385	27.5210
$V[m/s]$	0.8073	0.8292	2.1746	1.0000	0.8054	0.8073
$X_0[m]$	-883.9896	888.4642	1308.5299	1.0000	-884.2139	-883.9896
$Y_0[m]$	140.3387	141.6894	1308.1491	1.0000	140.8068	140.3387
$Z_0[m]$	2357.2826	2369.3341	1308.2852	0.0000	2357.4535	2357.2826
$X_P[m]$	-860.6125	865.1302	1308.5299	1.0000	-838.5421	-860.6125
$Y_P[m]$	142.7640	143.9917	1308.1491	1.0000	143.6613	142.7640
$Z_P[m]$	2343.3290	2355.5190	1308.2852	0.0000	2330.0504	2343.3290

Table 4.6 Simulation 2 Statistics Averaged For All 100 INS Runs

Sim 2	$\bar{e}_{\hat{X}^+}$	$\hat{\sigma}^+_{E_X}$	$\hat{\sigma}^+_X$	$P_{E_{1-\sigma}}$	INS_{err}	$\hat{X}_{err}$
$R[m]$	-3.0360	77.7768	69.7914	0.5731	-1.7734	-3.0360
$V[m/s]$	-0.0704	1.9599	2.0544	0.6250	-0.0701	-0.0704
$X_0[m]$	-2.4305	117.2956	110.1955	0.5253	-2.3933	-2.4305
$Y_0[m]$	1.4918	129.3327	106.0832	0.4621	1.2860	1.4918
$Z_0[m]$	-8.2071	133.8229	107.5727	0.5019	-7.8166	-8.2071
$X_P[m]$	-4.8080	129.7924	110.1955	0.4761	-3.9119	-4.8080
$Y_P[m]$	0.9270	129.4990	106.0832	0.4691	1.1911	0.9270
$Z_P[m]$	-5.9550	133.5656	107.5727	0.5419	-6.9055	-5.9550

Table 4.7 Simulation 2 Statistics For One Run

Sim 2	$\bar{e}_{\hat{X}^+}$	$\hat{\sigma}^+_{E_X}$	$\hat{\sigma}^+_X$	$P_{E_{1-\sigma}}$	INS_{err}	$\hat{X}_{err}$
$R[m]$	79.1916	89.1073	69.7742	0.4300	51.1091	79.1916
$V[m/s]$	2.4513	2.4941	2.0546	0.1300	2.4286	2.4513
$X_0[m]$	170.7278	171.6297	110.1949	0.0000	171.1893	170.7278
$Y_0[m]$	-21.0121	25.7675	106.0831	1.0000	-21.4275	-21.0121
$Z_0[m]$	-45.4545	54.3677	107.5673	0.9800	-42.7755	-45.4545
$X_P[m]$	241.0125	242.5320	110.1949	0.0000	214.9522	241.0125
$Y_P[m]$	-17.5077	23.3563	106.0831	1.0000	-18.6923	-17.5077
$Z_P[m]$	-81.7135	89.4990	107.5673	0.7900	-69.0332	-81.7135

Table 4.8 Simulation 3 Statistics Averaged For All 100 INS Runs

Sim 3	$\bar{e}_{\hat{X}^+}$	$\hat{\sigma}^+_{E_X}$	$\hat{\sigma}^+_X$	$P_{E_{1-\sigma}}$	INS_{err}	$\hat{X}_{err}$
$R[m]$	-4.6488	82.1057	73.8012	0.5895	-6.4591	-4.6488
$V[m/s]$	-0.1432	1.9762	2.1753	0.6305	-0.1381	-0.1432
$X_0[m]$	-153.0414	1360.6116	1308.5302	0.5299	-153.0519	-153.0414
$Y_0[m]$	-168.6607	1517.3375	1308.1476	0.4700	-168.6636	-168.6607
$Z_0[m]$	-366.9343	1593.8858	1308.2856	0.4593	-367.1790	-366.9343
$X_P[m]$	-157.3944	1370.1465	1308.5302	0.5300	-158.5905	-157.3944
$Y_P[m]$	-168.6664	1517.4836	1308.1476	0.4700	-168.6636	-168.6664
$Z_P[m]$	-364.8245	1591.1006	1308.2856	0.4595	-363.8558	-364.8245

Table 4.9 Simulation 3 Statistics For One Run

Sim 3	$\bar{e}_{\hat{X}^+}$	$\hat{\sigma}^+_{E_X}$	$\hat{\sigma}^+_X$	$P_{E_{1-\sigma}}$	INS_{err}	$\hat{X}_{err}$
$R[m]$	19.4617	47.7644	73.8134	0.8900	29.6816	19.4617
$V[m/s]$	0.5077	0.5478	2.1752	1.0000	0.5176	0.5077
$X_0[m]$	4255.7397	4277.1853	1308.5302	0.0000	4255.3422	4255.7397
$Y_0[m]$	-230.4375	231.5985	1308.1476	1.0000	-230.2658	-230.4375
$Z_0[m]$	-1441.2979	1448.9120	1308.2855	0.0000	-1442.6714	-1441.2979
$X_P[m]$	4270.8303	4292.3689	1308.5302	0.0000	4280.7939	4270.8303
$Y_P[m]$	-230.0941	231.2533	1308.1476	1.0000	-230.2658	-230.0941
$Z_P[m]$	-1453.5762	1461.5416	1308.2855	0.0000	-1457.9424	-1453.5762

Tables 4.4 through 4.9 provide two key observations into INS aiding using passive, bearings-only measurements of an unknown ground object. First, all three simulations show that the accuracy of $\hat{X}$ is driven by the accuracy of the INS measurements. Second, the unknown ground object's location is directly related to the accuracy of the INS-measured initial aircraft position. These two key observations show that INS aiding using an unknown ground object does not provide adequate information to enhance the aiding of the INS to produce better estimates of the initial position of the aircraft and the position of the ground object. The reasons behind this are evident in Figure 4.5. Figure 4.5 shows an example of the flight

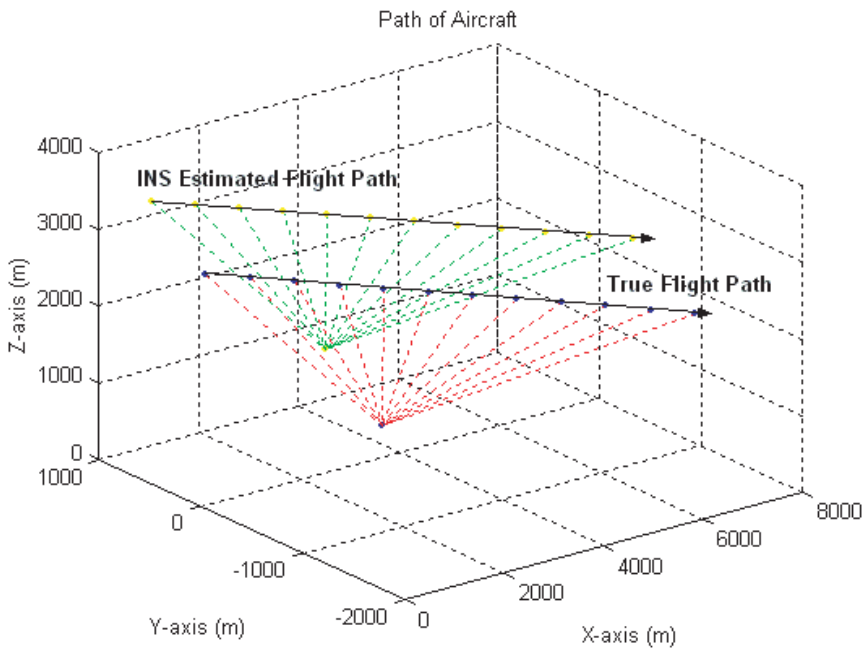

Figure 4.5 Flight Comparison Profile Plot

profiles generated from the initial INS measurements and the true location of the aircraft. Note that the drift of the INS is ignored. The flight path is generated using the initial INS measured position, velocity, heading, and flight path of the aircraft. The errors in the heading and the flight path angle are small; therefore, the flight paths appear to be parallel to each other. The initial INS-measured aircraft position augmented with the bearings-only measurements produce a measurement geometry

oriented parallel to the plane P in the true case, but offset due to the error in the initial INS measurement. Without prior knowledge of the unknown ground object's location in at least one inertial axis, there is no useful information to aid the INS. The offset of the unknown ground object is directly related to error in the initial INS measurement. The one advantage to using bearings-only measurements of an unknown ground object to aid the INS is that they maintain the initial accuracy of the INS throughout the entire measurement interval. This is because the aiding scheme uses the newly estimate initial position in conjunction with the flight path angle, the heading, and the velocity of the aircraft to generate an aiding point as described in Section 4.3. Thus, no matter how much the INS drifts over time, the navigation solution will reflect the initial INS measurement errors. This is particularly useful for a tactical-grade INS that has lost aiding information from an external source like GPS. The bearings-only measurement aiding algorithm maintains the accuracy of the navigation system at the point of losing that external source, or until the external source is able to aid the INS again.

The inability of bearings-only measurements of an unknown ground object to aid the INS is a major drawback; however, the ability to maintain the navigation system's accuracy over very long periods of time is very advantageous. This aiding concept coupled with GPS aiding produces a navigation system that does not divulge the presence of the aircraft while maintaining a high degree of accuracy even when the GPS signal is lost or jammed. The next section examines the effectiveness of the aiding algorithm, given prior information on the ground object.

4.6.3 Tactical-Grade INS, Given Prior Information. Prior information on the location of the ground object should greatly enhance the accuracy of the aiding algorithm. The first two simulations in Scenario 1 were repeated, but with prior knowledge of the position of the ground object in the inertial frame. Although this modifies the aiding concept to bearings-only measurements of a *known* ground object, the passive nature of the aiding system is preserved because no measured

range information is being used to enhance the aiding algorithm. Tables 4.10 and 4.11 show the statistics for the modified first run in Scenario 1. Tables 4.12 and 4.13 show the statistics for the modified second run in Scenario 1. The error in the prior information is modeled as a normal distribution with zero-mean and standard deviation of 10 meters in the horizontal and vertical channels. These error values reflect the accuracy of a standard GPS receiver.

Table 4.10 Simulation 1 Statistics Averaged For All 100 INS Runs

Sim 1	$\bar{e}_{\hat{X}^+}$	$\hat{\sigma}^+_{E_X}$	$\hat{\sigma}^+_X$	$P_{E_{1-\sigma}}$	INS_{err}	$\hat{X}_{err}$
$R[m]$	8.9195	83.2175	73.8522	0.5714	6.9096	8.9195
$V[m/s]$	0.2560	2.0492	2.1737	0.6186	0.2615	0.2560
$X_0[m]$	-7.3544	62.1996	64.0239	0.6157	3.1331	-7.3544
$Y_0[m]$	-0.7367	31.0333	10.7828	0.2720	39.9037	-0.7367
$Z_0[m]$	4.6980	75.9530	39.2640	0.3906	4.1329	4.6980
$X_P[m]$	0.0207	9.9670	9.9999	0.6846	0.7032	0.0207
$Y_P[m]$	-0.0455	9.9344	9.9999	0.6863	-0.4214	-0.0455
$Z_P[m]$	0.0556	10.0272	9.9999	0.6816	0.3877	0.0556

Table 4.11 Simulation 1 Statistics For One Run

Sim 1	$\bar{e}_{\hat{X}^+}$	$\hat{\sigma}^+_{E_X}$	$\hat{\sigma}^+_X$	$P_{E_{1-\sigma}}$	INS_{err}	$\hat{X}_{err}$
$R[m]$	46.7922	61.9107	73.8177	0.7600	36.9927	46.7922
$V[m/s]$	1.5414	1.5755	2.1740	0.9800	1.4459	1.5414
$X_0[m]$	-42.6711	45.4843	64.0709	0.9200	-1779.9409	-42.6711
$Y_0[m]$	0.8276	32.1606	10.7966	0.3000	2965.1303	0.8276
$Z_0[m]$	17.3159	67.1942	39.4343	0.4300	205.8037	17.3159
$X_P[m]$	0.2901	8.8727	9.9999	0.7900	-5.8352	0.2901
$Y_P[m]$	0.3795	9.3127	9.9999	0.6900	4.3586	0.3795
$Z_P[m]$	-1.8267	10.3240	9.9999	0.7000	-8.5855	-1.8267

Table 4.12 Simulation 2 Statistics Averaged For All 100 INS Runs

Sim 2	$\bar{e}_{\hat{X}^+}$	$\hat{\sigma}^+_{E_X}$	$\hat{\sigma}^+_X$	$P_{E_{1-\sigma}}$	INS_{err}	$\hat{X}_{err}$
$R[m]$	-5.3719	72.7449	66.3281	0.5770	-3.0583	-5.3719
$V[m/s]$	-0.1654	1.9246	1.9523	0.5928	-0.1524	-0.1654
$X_0[m]$	4.9721	55.0434	57.4265	0.5988	18.1146	4.9721
$Y_0[m]$	0.1072	30.5194	10.6171	0.2808	-22.5790	0.1072
$Z_0[m]$	-2.6467	70.3398	35.4206	0.3808	15.6912	-2.6467
$X_P[m]$	0.0182	9.9776	9.9810	0.6849	-0.1499	0.0182
$Y_P[m]$	-0.0328	10.0367	9.9779	0.6828	0.3477	-0.0328
$Z_P[m]$	-0.1090	9.9544	9.9790	0.6792	-0.0982	-0.1090

Table 4.13 Simulation 2 Statistics For One Run

Sim 2	$\bar{e}_{\hat{X}^+}$	$\hat{\sigma}^+_{E_X}$	$\hat{\sigma}^+_X$	$P_{E_{1-\sigma}}$	INS_{err}	$\hat{X}_{err}$
$R[m]$	-39.9856	47.8810	66.3422	0.8100	-30.9979	-39.9856
$V[m/s]$	-1.2798	1.3517	1.9520	0.9600	-0.4479	-1.2798
$X_0[m]$	35.0452	37.7863	57.4238	0.9600	168.2128	35.0452
$Y_0[m]$	0.1761	25.7942	10.6147	0.3100	-279.2516	0.1761
$Z_0[m]$	-20.0517	54.2174	35.3763	0.4600	-48.1773	-20.0517
$X_P[m]$	0.1419	9.7571	9.9810	0.7000	-2.0361	0.1419
$Y_P[m]$	-0.7471	9.8139	9.9779	0.7000	1.5579	-0.7471
$Z_P[m]$	-0.2374	9.5265	9.9790	0.6900	-12.6106	-0.2374

The inclusion of prior information on the position of the ground object greatly enhances the parameter estimate provided by the aiding algorithm. The accuracy of the algorithm is comparable to that of an integrated GPS/INS system in which the errors in the navigation solution are driven by the accuracy of the GPS receiver. The current generation of GPS receivers provide position estimates to within 10 meters in the horizontal channel and 15 meters in the vertical channel [5]. The comparable statistics are due, in no small part, to the accuracy in the known location of the ground object which is similar to that of a standard GPS receiver. The major roadblock to producing very accurate estimates of the parameter X comes from the estimation of the initial range R. The estimate of the initial range R is based solely on geometry and the accuracy in the measured angle σ, the calculated angle γ_D, and

the distance the aircraft covers in the first measurement interval. This produces an estimate of R that is in error anywhere between 50 and 150 or more meters. This is based on what was observed over may different simulation scenarios. A very accurate estimation of the initial range from a laser range finder would produce very accurate estimates of the parameter X, but at the cost of sacrificing the passive nature of the aiding scheme.

4.6.4 Low/High Altitude Scenarios. Scenarios 1 and 2 provide good insight into the feasibility of using passive, bearings-only measurements of unknown or known stationary ground objects to aid the aircraft's INS. The two previous scenarios took into consideration the importance prior ground information has on the output of the aiding algorithm. They also show how the accuracy of the initial INS measurement and the accuracy of prior ground object information affect the estimated parameter $\hat{X}$. The one key consideration Scenarios 1 and 2 ignore, is the role measurement geometry plays in the aiding scheme. From here on, the Geometric Dilution of Precision (GDOP) of the bearings-only INS aiding scheme is used to describe favorable or unfavorable measurement geometry. A high GDOP will not produce accurate parameter estimates, while a low GDOP will. Altitude, velocity, and measurement time greatly effect the magnitude of the angle recorded between measurement intervals. Small measurements of σ produce a poor calculation of γ_D. This is because the magnitude of the σ measurements are equal to or less than the magnitude of the noise corrupting those measurements, thus producing measurements with seemingly large errors. The bearings-only σ measurements are a key factor in calculating γ_D, and measurements with seemingly large errors produce a poor calculation of γ_D. This, in turn, corrupts the geometric property used to estimate the range R and could have a devastating impact on the accuracy of the aiding algorithm. The previous two scenarios contained measurement times intervals of four seconds, more than adequate to produce good "clean" σ measurements.

"Clean" refers to measurements of σ that have a high Signal-To-Noise Ratio (SNR), thus producing a very accurate calculation of γ_D.

Table 4.14 shows the parameters of the three simulations that were run for the third scenario. As in the second scenario, Scenario 3 assumes prior information on

Table 4.14 Scenario Parameters

	Sim 1	Sim 2	Sim 3
$V[m/s]$	200	200	150
$\gamma[deg]$	0	0	0
$H[deg]$	-10	-10	5
$X_0[m]$	0	0	0
$Y_0[m]$	0	0	0
$Z_0[m]$	20000	20000	500
$X_P[m]$	4000	20000	500
$Y_P[m]$	300	300	0
$Z_P[m]$	200	200	200
$t[s]$	1	12	0.5
N	12	12	12

the ground object's location is available. Table 4.15 shows the INS measurement errors for each of the simulations. The first simulation is based on a high altitude

Table 4.15 INS Errors - $\mathcal{N}(0, \sigma_N^2)$

	$1-\sigma$	$1-\sigma$	$1-\sigma$
$V[m/s]$	2.5	2.5	2.5
$\gamma[deg]$	1e-4	1e-4	1e-4
$H[deg]$	1e-4	1e-4	1e-4
$X_0[m]$	1850	1850	1850
$Y_0[m]$	1850	1850	1850
$Z_0[m]$	1850	1850	1850

reconnaissance mission flown by aircraft such as the U-2. The second simulation is the same as the first simulation but with a longer measurement interval, and the ground object is farther down range. The longer measurement interval produces an increased distance between the bearing measurement points. This should increase the

SNR of the σ measurement, thus enhancing the aiding capabilities of the navigation system. Tracking a ground object farther down range produces a lower GDOP. The third simulation is based on a low altitude reconnaissance UAV. All three simulations are using prior information on the ground object's location with the same errors outlined in the second scenario.

Tables 4.16 and 4.17 show the statistics for the first simulation. As noted earlier, the aided INS solution is very poor due to the low SNR of the bearings measurements and a high GDOP for the scenario. Figure 4.6 shows the measurement geometry for the first simulation.

Table 4.16 Simulation 1 Statistics Averaged For All 100 INS Runs

Sim 1	$\bar{e}_{\hat{X}^+}$	$\hat{\sigma}^+_{E_X}$	$\hat{\sigma}^+_X$	$P_{E_{1-\sigma}}$	INS_{err}	$\hat{X}_{err}$
$R[m]$	-19113.5466	19218.4868	14.3089	0.0000	-18729.6431	-19113.5466
$V[m/s]$	0.1864	12.7912	2.4884	0.1363	-0.1207	0.1864
$X_0[m]$	2992.3163	3015.1786	16.4114	0.0000	-17.6376	2992.3163
$Y_0[m]$	472.8255	476.7980	10.8937	0.0001	-276.3645	472.8255
$Z_0[m]$	-19706.6545	19816.4586	12.9606	0.0000	-118.8944	-19706.6545
$X_P[m]$	0.0268	10.0659	9.9999	0.6842	0.8614	0.0268
$Y_P[m]$	-0.1374	9.9438	9.9999	0.6819	0.3566	-0.1374
$Z_P[m]$	0.5633	10.0084	9.9999	0.6825	-0.0823	0.5633

Table 4.17 Simulation 1 Statistics For One Run

Sim 1	$\bar{e}_{\hat{X}^+}$	$\hat{\sigma}^+_{E_X}$	$\hat{\sigma}^+_X$	$P_{E_{1-\sigma}}$	INS_{err}	$\hat{X}_{err}$
$R[m]$	-19126.0231	19223.1137	13.3910	0.0000	-18431.2635	-19126.0231
$V[m/s]$	1.1912	9.6468	2.4900	0.1400	0.9507	1.1912
$X_0[m]$	2994.1408	3012.8153	16.1114	0.0000	1566.9345	2994.1408
$Y_0[m]$	475.9351	478.7531	10.2380	0.0000	-994.3409	475.9351
$Z_0[m]$	-19738.0377	19840.3674	12.0229	0.0000	-10.8293	-19738.0377
$X_P[m]$	2.5344	10.3581	9.9999	0.6800	14.6713	2.5344
$Y_P[m]$	1.2831	9.3906	9.9999	0.6700	11.8909	1.2831
$Z_P[m]$	1.5911	9.2636	9.9999	0.7100	-2.2517	1.5911

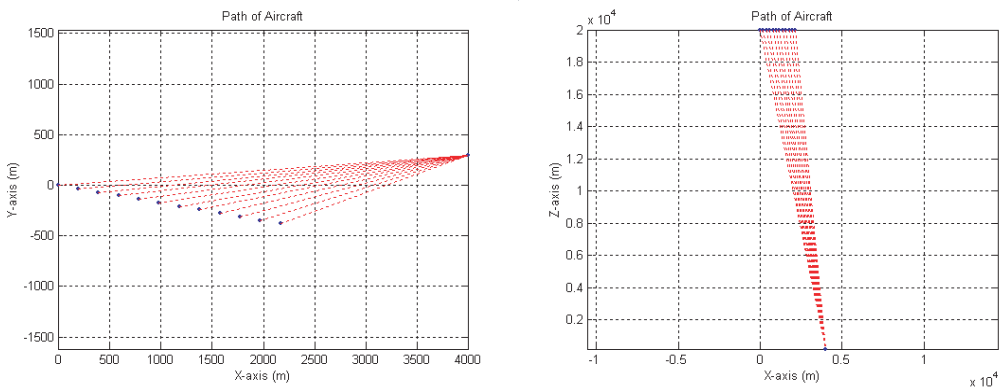

Figure 4.6 High GDOP Example

The triangles which construct the measurement geometry have small σ angles and are very similar in shape and size. This poor geometric relationship greatly degrades the effectiveness of Equation (3.39). Figure 4.7, on the other hand, shows the measurement geometry for a low GDOP. The flight profile in Figure 4.7 will

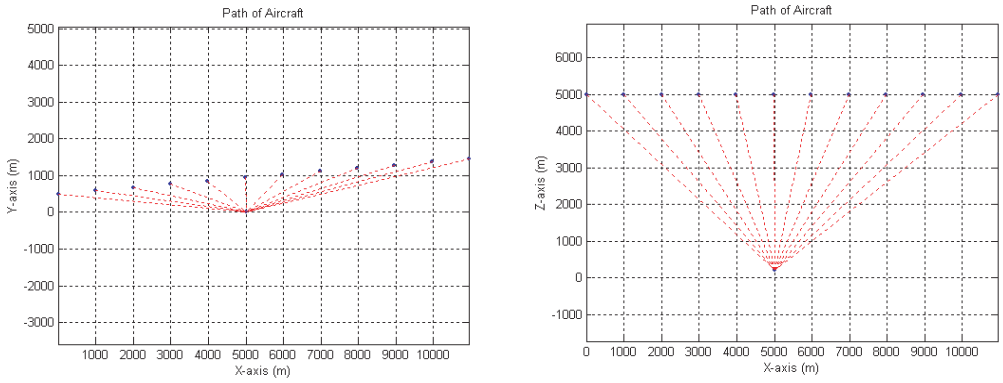

Figure 4.7 Low GDOP Example

produce very reliable position estimates because the bearings-only measurements have a very high SNR and the measurement geometry produces a low GDOP.

The problems regarding the low SNR and high GDOP in the first simulation stem from the short measurement interval used at such a high altitude, and the relatively low speed of the aircraft. There are two approaches available to produce σ measurements with a high SNR and a good GDOP at high altitudes. The first

approach is to increase the speed of the aircraft greatly to lengthen the measurement baseline; however, this approach is impractical for most aircraft operating at high altitudes, save the SR-71 Blackbird which is no longer in military service. The second approach is to increase the measurement time interval greatly.

Tables 4.18 and 4.19 show the statistics for the second simulation with a measurement interval twelve times greater than in the first simulation. The longer

Table 4.18 Simulation 2 Statistics Averaged For All 100 INS Runs

Sim 2	$\bar{e}_{\hat{X}+}$	$\hat{\sigma}^+_{E_X}$	$\hat{\sigma}^+_X$	$P_{E_{1-\sigma}}$	INS_{err}	$\hat{X}_{err}$
$R[m]$	-13.6394	351.5625	137.5949	0.2722	-10.9324	-13.6394
$V[m/s]$	-0.0938	3.4669	0.9780	0.2127	-0.0602	-0.0938
$X_0[m]$	12.0762	248.3450	137.9679	0.3740	74.2933	12.0762
$Y_0[m]$	0.3043	96.3025	35.6957	0.2000	142.2469	0.3043
$Z_0[m]$	-10.4683	439.5154	137.9731	0.2468	-35.5015	-10.4683
$X_P[m]$	-0.0132	10.0533	9.9999	0.6786	-0.7654	-0.0132
$Y_P[m]$	-0.0434	10.0405	9.9999	0.6804	0.5064	-0.0434
$Z_P[m]$	0.0304	9.9359	9.9999	0.6881	-0.4890	0.0304

Table 4.19 Simulation 2 Statistics For One Run

Sim 2	$\bar{e}_{\hat{X}+}$	$\hat{\sigma}^+_{E_X}$	$\hat{\sigma}^+_X$	$P_{E_{1-\sigma}}$	INS_{err}	$\hat{X}_{err}$
$R[m]$	26.0367	187.9943	137.6651	0.5300	16.4512	26.0367
$V[m/s]$	-0.4823	2.8122	0.9752	0.2400	-0.1342	-0.4823
$X_0[m]$	13.3759	142.9921	138.1183	0.6900	-3331.8097	13.3759
$Y_0[m]$	-14.0654	103.1738	10.6691	0.0800	706.3771	-14.0654
$Z_0[m]$	48.4386	397.0985	138.1501	0.2600	891.8619	48.4386
$X_P[m]$	-1.3528	10.3306	9.9999	0.6500	1.7228	-1.3528
$Y_P[m]$	-0.1419	9.5177	9.9999	0.7400	6.0435	-0.1419
$Z_P[m]$	0.5731	8.9910	9.9999	0.7000	0.2257	0.5731

measurement interval time does have a very positive impact on the estimate of the X parameter. The aiding algorithm is able to reduce the position errors a significant amount and produce a very accurate estimate of the initial aircraft position. The key factor in producing reliable position estimates at high altitudes is to use a long measurement interval to produce "clean" σ measurements.

Tables 4.20 and 4.21 show the statistics for the third simulation at a low altitude with a very short measurement interval. Even with a measurement time interval of

Table 4.20 Simulation 3 Statistics Averaged For All 100 INS Runs

Sim 3	$\bar{e}_{\hat{X}+}$	$\hat{\sigma}^+_{E_X}$	$\hat{\sigma}^+_X$	$P_{E_{1-\sigma}}$	INS_{err}	$\hat{X}_{err}$
$R[m]$	-0.5379	8.1914	9.6978	0.6967	-0.6585	-0.5379
$V[m/s]$	-0.1382	2.0101	2.4947	0.7100	-0.1387	-0.1382
$X_0[m]$	0.5097	12.7426	13.0909	0.6865	-93.7232	0.5097
$Y_0[m]$	0.0836	10.1460	10.9601	0.6886	-71.6735	0.0836
$Z_0[m]$	-0.2890	11.5214	11.4492	0.6813	-8.1869	-0.2890
$X_P[m]$	0.0393	10.1735	9.9999	0.6777	0.0325	0.0393
$Y_P[m]$	0.0738	10.0352	9.9999	0.6801	0.6352	0.0738
$Z_P[m]$	-0.0139	9.9875	9.9999	0.6886	-0.3097	-0.0139

Table 4.21 Simulation 3 Statistics For One Run

Sim 3	$\bar{e}_{\hat{X}+}$	$\hat{\sigma}^+_{E_X}$	$\hat{\sigma}^+_X$	$P_{E_{1-\sigma}}$	INS_{err}	$\hat{X}_{err}$
$R[m]$	-7.0550	7.3378	9.7005	0.9600	-8.3736	-7.0550
$V[m/s]$	-1.8554	1.8648	2.4947	1.0000	-1.8631	-1.8554
$X_0[m]$	6.5723	12.8479	13.0888	0.7300	-363.0662	6.5723
$Y_0[m]$	1.8937	12.0105	9.9999	0.5400	3543.2999	1.8937
$Z_0[m]$	-1.5253	10.7921	11.4456	0.7100	1540.2150	-1.5253
$X_P[m]$	0.3468	11.1030	9.9999	0.6800	1.3087	0.3468
$Y_P[m]$	1.9415	12.0042	9.9999	0.5400	-18.2006	1.9415
$Z_P[m]$	1.8273	9.9613	9.9999	0.6800	4.0174	1.8273

only half a second, low altitude aiding produces a very good estimate of the aircraft's initial position. This is due to the high SNR of the σ measurements and the low GDOP of the bearings-only measurements.

The SNR for the three simulations is calculated ad hoc by dividing the power of the received signal (initial σ measurement) by the power of the corrupting noise (assumed to be 5e-4 rad). The ad hoc method provides a simple means of comparing the SNR for each of the three simulations in Scenario 3. The SNR for the first simulation is 19.47, while the SNR for the second simulation is 129.68. The increased measurement time for the second simulation greatly increases the SNR of the σ

measurement. The SNR for the third simulation is 149.97. It is clearly evident that the SNR of the initial σ measurement plays a key role in the accuracy of the estimated parameters, and that low altitude aiding appears to produce the best parameter estimates. Calculation of a GDOP value for the three simulations is extremely complicated for this particular application, and thus is handled ad hoc by examination of Figures 4.6 and 4.7 as discussed earlier. Figure 4.7 undoubtedly has a better measurement geometry than that of Figure 4.6, thus producing a lower GDOP and more accurate parameter estimates.

4.7 Discussion

INS aiding using passive, bearings-only measurements over time of an unknown, but stationary ground object, provides a means to enhance the aircraft's attitude estimate. The INS aiding method does not significantly enhance the positional navigation variables' accuracy unless prior knowledge of the position of the observed ground object is available; however, it does maintain the accuracy of the INS over the measurement interval, thus performing a "damping" function. The two key factors in producing reliable aiding information for the INS are high signal-to-noise ratios for the LOS measurements and a low GDOP measurement scenario. Inclusion of prior information on the location of the ground object greatly enhances the accuracy of the aiding algorithm, but somewhat changes the nature of the aiding scheme. Without prior information, the accuracy of the aiding algorithm directly correlated to the error in the initial INS measurement, while prior information on the ground object's location provided enhanced aiding to the INS. Prior information or not, the aiding algorithm is dependent solely on bearings-only measurements, thus maintaining the autonomy of the INS and the passive nature of the navigation system.

V. Conclusions and Recommendations

5.1 Conclusions

INS aiding using passive, bearings-only measurements over time of an unknown, but stationary ground object is investigated. The aiding concept is based on the relationships of the measured α' and β' angles between the aircraft's inertial velocity vector $\vec{V}$ and the body of the aircraft, to the five angular navigation variables ψ, θ, ϕ, γ, and H, and stadiametry. The theory developed herein also allows for the inclusion of additional measurements and prior information, i.e., the aircraft's baro-altitude, the range to the ground object, and any information on the position of the ground object, if available.

The major disadvantage of a stand alone bearings-only measurement based INS aiding scheme is that it does not produce a significantly better estimate of the aircraft's position. It does however, produce enhanced estimates of the aircraft's angular navigation variables viz., the aircraft's attitude, and the ground object is geo-located. For the aiding scheme to also enhance the accuracy of the aircraft's positional variables' estimates, prior information on the location of the ground object is required, in which case the improvement in positional accuracy is significant. Baro-altitude information and optical measurements can enhance the aircraft's position estimate. Also, the INS aiding scheme does maintain the accuracy of the INS, thus successfully performing an INS damping function.

The aircraft must be flown at a constant velocity and maintain its course and heading while taking bearings-only measurements to perform the INS aiding function. While a limitation, this is not a serious enough limitation to render the system operationally unacceptable. This type of system could act as a redundant navigation tool for an integrated GPS/INS navigation system. If the GPS signal is lost or jammed, bearings-only measurements would maintain the overall accuracy of the integrated solution until the GPS signal is reacquired. The major advantage of

the aiding scheme is that it creates a fully integrated and autonomous navigation system impervious to jamming, spoofing, or interference, and without giving away the aircraft's presence.

While stand alone bearings-only measurements/optical flow measurement over time turn out to be a "weak" measurement in itself, when used in conjunction with the INS measurements, it proves to be most beneficial. In the case regarding an unknown stationary landmark, it maintains the accuracy of the initial INS measurement, in effect negating the drift of the INS over time. In the case regarding a known stationary ground object, it greatly enhances the estimate of the aircraft's position variables producing very reliable navigation information.

5.2 Recommendations

This study thoroughly describes the process of using passive, bearings-only measurements of an unknown, but stationary, ground object to aid an aircraft's INS. Further research in this area could extend into a real-time aiding system adapted from current optical, or electro-optical sensors. This would require a more robust algorithm designed to operate outside a controlled laboratory environment.

The next evolution in this field of study is to develop the theory for the operation of the algorithm under dynamic environments. Dynamic environments would require a more flexible aiding scheme using techniques such as Kalman filtering, extended Kalman filtering, or Multiple Model Adaptive Estimation (MMAE) techniques. This would allow the aiding scheme to operate during mild maneuvers and not be restricted to linear flight.

Bibliography

1. *Space Navigation Guidance and Control, Report R-500*. Technical Report, MIT Instrumentation Laboratory, 1965.
2. Andrew, William J.H. and Dava Sobel. *The Illustrated Longitude*. New York: Walker and Company, 1998.
3. Boiffier, Jean-Luc. *The Dynamics of Flight The Equations*. England: John Wiley & Sons, 1998.
4. Maybeck, Peter S. *Stochastic Models, Estimation and Control Volume 1*. Virginia: Navtech Book & Software Store, 1994.
5. Misra, Pratap and Per Enge. *Global Positioning System Signals, Measurements, and Performance*. Massachusetts: Ganga-Jamuna Press, 2001.
6. Pachter, Meir. "INS Aiding By Using Optical Flow." To be presented at the 2003 American Control Conference.
7. Polat, Murat. *INS Aiding By Tracking An Unknown Ground Object*. MS Thesis, AFIT/GE/ENG/02M-20, School of Engineering, Air Force Institute of Technology, Wright-Patterson AFB OH, March 2002 (ADA-401452).
8. Rogers, Robert M. *Applied Mathematics in Integrated Navigation Systems*. Virginia: American Institute of Aeronautics and Astronautics, Inc., 2000.
9. Siouris, George M. *Aerospace Avionics Systems, A Modern Synthesis*. Virginia: Academic Press, Inc., 1993.
10. Titterton, D.H. and J.L. Weston. *Strapdown Inertial Navigation Technology*. IEE, 1997.
11. Van Sickle, N.D. *Modern Airmanship*. New Jersey: D. Van Nostrand Company, INC., 1957.

REPORT DOCUMENTATION PAGE

Form Approved
OMB No. 074-0188

1. REPORT DATE *(DD-MM-YYYY)*	2. REPORT TYPE	3. DATES COVERED *(From – To)*
25-03-2003	**Master's Thesis**	October 2001 – March 2003

4. TITLE AND SUBTITLE

INS AIDING USING PASSIVE, BEARINGS-ONLY MEASUREMENTS OF AN UNKNOWN STATIONARY GROUND OBJECT

5a. CONTRACT NUMBER

5b. GRANT NUMBER

5c. PROGRAM ELEMENT NUMBER

6. AUTHOR(S)

Porter, Alec E., Second Lieutenant, USAF

5d. PROJECT NUMBER

5e. TASK NUMBER

5f. WORK UNIT NUMBER

7. PERFORMING ORGANIZATION NAMES(S) AND ADDRESS(S)
Air Force Institute of Technology
Graduate School of Engineering and Management (AFIT/EN)
2950 Hobson Way, Building 640
WPAFB OH 45433-7765

8. PERFORMING ORGANIZATION REPORT NUMBER

AFIT/GE/ENG/03-15

9. SPONSORING/MONITORING AGENCY NAME(S) AND ADDRESS(ES)
AFRL\MNGN(AFMC)
Attn: Major Ryan Pendleton
Air Force Research Lab, Munitions Directorate DSN: 872-9443 x 1290
Eglin AFB, FL 32542 e-mail:ryan.pendleton@eglin.af.mil

10. SPONSOR/MONITOR'S ACRONYM(S)

11. SPONSOR/MONITOR'S REPORT NUMBER(S)

12. DISTRIBUTION/AVAILABILITY STATEMENT

APPROVED FOR PUBLIC RELEASE; DISTRIBUTION UNLIMITED.

13. SUPPLEMENTARY NOTES

14. ABSTRACT
The theory for Inertial Navigation System (INS) aiding using passive, bearings-only measurements of an unknown ground object, in the vein of optical flow measurement, is developed. Stand-alone bearings-only measurements over time of an unknown, but stationary, ground object are shown to yield estimates of the aircraft's aerodynamic angles, viz., the angle of attack and sideslip angle. Two new equations containing the aircraft's angular navigation variables ψ, θ, φ, γ, H, and the aerodynamic angles are derived. This allows an update of the aircraft's baro-attitude, thus making INS aiding using passive, bearings-only measurements possible. Moreover, the use of stadiametry, knowledge of the ground object's elevation, and an independent altitude measurement yields an improved estimate of the aircraft's positional variables, thus completing the INS aiding task. At the same time, the geo-location of the observed ground object is also obtained. In addition, prior information on the position of the ground object further enhances the positional navigation variables' estimate, thus bringing to full fruition the favorable synergy of INS and bearings-only measurements of an unknown ground object.

15. SUBJECT TERMS
Inertial Navigation Aiding, Passive Tracking, Estimation.

16. SECURITY CLASSIFICATION OF:			17. LIMITATION OF ABSTRACT	18. NUMBER OF PAGES	19a. NAME OF RESPONSIBLE PERSON
a. REPORT	b. ABSTRACT	c. THIS PAGE			Dr. Pachter, Meir, Professor
U	U	U	UU	90	19b. TELEPHONE NUMBER *(Include area code)* (937) 255-3636, ext 4593; e-mail: Meir.Pachter@afit.edu